

$p=0.0174$ ). No significant differences in all other clinical and laboratory data were found between the 2 groups (Table 2).

We also analyzed all sequences of *MEFV* genes in normal Japanese subjects ( $n=62$ ). These individuals were healthy adult volunteers and had no recurrent episodes of fever. There was no difference in recruitment between the PFAPA patients and the control group. A comparison of these results between normal and PFAPA subjects is shown in Table 3. In normal individuals, no significant allele frequencies were observed for the 4 variants found in PFAPA patients. In addition, the frequencies of *E148Q-L110P* and *P369S-R408Q* in the 2 groups were compared. A significant difference in the frequency of these variants was observed between the 2 groups (Table 4,  $p = 0.043$  and  $p = 0.026$ , respectively).

**Table 3. Allele Frequencies of *MEFV* Variants in PFAPA Subjects and Normal Unaffected Subjects**

Variant	PFAPA Subjects (n=40)	Unaffected Subjects (n=124)	P Value
<i>E148Q</i>	30.0%	18.5%	NS
<i>L110P</i>	17.5%	6.5%	NS
<i>G304R</i>	0.0%	3.2%	NS

NS: not significant.

**Table 4. Frequencies of *MEFV* Variants in PFAPA Subjects and Normal Unaffected Subjects**

Variant	PFAPA Subjects (n=20)	Unaffected Subjects (n=62)	P Value
<i>E148Q-L110P</i>	35%	13%	$P=0.043$

## DISCUSSION

We studied 20 patients with PFAPA who were diagnosed by Marshall criteria [1]. Our aim was to access the roles of the predominant variants in genes that cause other febrile illnesses like FMF, TNF receptor-associated periodic syndrome (TRAPS) and the MVK deficiency. We did not find any incidence of variants of TRAPS and MVK deficiency in PFAPA patients. However several heterogeneous variants of *MEFV* were detected in 13 out of 20 patients with PFAPA. We analyzed the frequency of the *E148Q-L110P* and *P369S-R408Q* variants in PFAPA and control subjects. Our analyses indicate that the incidence of these 2 variants is significantly higher in patients with PFAPA than in normal individuals.

Amongst autoinflammatory disease, only PFAPA syndrome has been described as a non-inherited syndrome, since familial inheritance has not been reported in previous studies [3,12,13]. However some studies have reported familial cases that included siblings or a sibling and the sibling's mother [14-16]. Therefore, the hereditary nature of this syndrome is still a matter of debate. With respect to the genetic factors that may cause the PFAPA syndrome, one study has strongly argued against the involvement of the *MEFV* gene [10], but another article [11] has shown that mutations of the *MEFV* genes were found in 27% of cases diagnosed with PFAPA syndrome on the basis of Marshall's

clinical criteria. Our observations of the high frequency (65%) of *MEFV* variants are in agreement with that reported by Dagan [11]. The differences in the findings may be attributed to the ethnic differences between the individuals studied, the small sized of the study, and the study population that was selected.

The *L110P* variant, which is located in exon 2, was first reported in FMF patients in 2000 [17], and to date, several compound heterozygotes with other variants have been reported even in Japan [18,19]. In contrast, although the role of the *E148Q* variant, which is located in exon 2, in FMF patients was controversial, a recent study concluded that the variant is just a benign polymorphism [20]. In a Japanese study [18] of FMF patients, the most frequently observed *MEFV* variants observed were *E148Q/M694I* (25.0%), *M694I* (17.5%), and *L110P/E148Q/M694I* (17.5%). However, no patients had the *M694V* variant. These patterns are quite different from those in Mediterranean patients with FMF. The study also reported that the allele frequencies of *E148Q*, *M694I*, and *L110P* were 0.44, 0.35, and 0.31, respectively, and that these frequencies were significant difference from those seen in healthy controls. In our study, the allele frequencies of *E148Q*, *L110P*, and *G304* were 0.3, 0.175, and 0, respectively, and these frequencies did not differ significantly between patients and healthy controls. No mutation at the *M694I* was detected in our cohorts of patients and controls. The allele frequency of *L110P* is higher in patients with PFAPA than in healthy controls; however, the difference is not significant. The frequency of the *E148Q-L110P* variant combination is significantly higher in the PFAPA group than in the healthy control group. If the *E148Q* variant is non-functional, the *L110P* variant may be associated with the onset of PFAPA syndrome.

In several types of inflammatory such as Behcet's disease [21], Crohn's disease [22], ulcerative colitis [23], Henoch-Schönlein purpura [24,25] and the co-incidence of FMF variants has been investigated. These studies show increased incidence of genes involved in FMF in patients with these autoinflammatory diseases as well as the increased severity of the symptoms of each disease. On the other, in the patients with asthma, the incidence of FM mutation was decreased and the lower incidence correlated with reduced severity of symptoms [26]. Thus, FMF variants may affect the transition from Th2 to Th1 polarity in each disease. According to Berkun's study [27], PFAPA episodes in carriers of *MEFV* variants were shorter compared to those in patients without variants. In *MEFV* variant-positive patients, the regular cyclic pattern of attacks and the occurrence of oral aphthae was lower than those in patients without *MEFV* variants. In the present study, we found that the only affected variable was the duration of PFAPA episodes. Although no significant differences were observed in the regular cyclic pattern of attacks and the occurrence of oral aphthae between the 2 groups, the duration of PFAPA episodes was shorter in the variant-positive group than in the variant-negative group.

Taken together, these results show that the *MEFV* gene may not affect the onset of several autoinflammatory diseases, but is likely to modify the intensity and the displayed phenotype in terms of disease symptoms.

In conclusion, the *MEFV* variants, viz. *E148Q-L110P*, *P369-R408Q* may be associated with the onset of PFAPA, and some *MEFV* variants may affect the phenotype of PFAPA.

### CONFLICT OF INTEREST

The authors confirm that this article content has no conflict of interest.

### ACKNOWLEDGEMENTS

The study was supported by the Mami Mizutani Foundation.

### REFERENCES

- [1] Marshall GS, Edwards KM, Lawton AR. PFAPA syndrome. *Pediatr Infect Dis J* 1989; 8: 658-9.
- [2] Wurster VM, Carlucci JG, Feder HM Jr, Edwards KM. Long-term follow-up of children with periodic fever, aphthous stomatitis, pharyngitis, and cervical adenitis syndrome. *J Pediatr* 2011; 159: 958-64.
- [3] Thomas KT, Feder HM Jr, Lawton AR, Edwards KM. Periodic fever syndrome in children. *J Pediatr* 1999; 135: 15-21.
- [4] Feder HM, Salazar JC. A clinical review of 105 patients with PFAPA (a periodic fever syndrome). *Acta Paediatr* 2010; 99: 178-84.
- [5] The International FMF Consortium. Ancient missense mutations in a new member of the RoRet gene family are likely to cause familial Mediterranean fever. *Cell* 1997; 90: 797-807.
- [6] French FMF Consortium. A candidate gene for familial Mediterranean fever. *Nat Genet* 1997; 17: 25-31.
- [7] Medlej-Hashim M, Loiselet J, Lefranc G, Mègarbané A. [Familial Mediterranean Fever (FMF): from diagnosis to treatment. *Sante* 2004; 14: 261-6.
- [8] Soyomezoglu O, Arga M, Fidan K, *et al.* Unresponsiveness to colchicine therapy in patients with familial Mediterranean fever homozygous for the M694V mutation. *J Rheumatol* 2010; 37: 182-9.
- [9] Padeh S, Brezniak N, Zemer D, *et al.* Periodic fever, aphthous stomatitis, pharyngitis, and adenopathy syndrome: clinical characteristics and outcome. *J Pediatr* 1999; 135: 98-101.
- [10] Cazeneuve C, Geneviève D, Amselem S, Hentgen V, Hau I, Reinert P. *MEFV* gene analysis in PFAPA. *J Pediatr* 2003; 143: 140-1.
- [11] Dagan E, Gershoni-Baruch R, Khatib I, Mori A, Brik R. *MEFV*, *TNFR1A*, *CARD15* and *NLRP3* mutation analysis in PFAPA. *Rheumatol Int* 2010; 30: 633-6.
- [12] Feder HM Jr, Bialecki CA. Periodic fever associated with aphthous stomatitis, pharyngitis and cervical adenitis. *Pediatr Infect Dis J* 1989; 8: 186-7.
- [13] Tasher D, Somekh E, Dalal I. PFAPA syndrome: new clinical aspects disclosed. *Arch Dis Child* 2006; 91: 981-4.
- [14] Sampaio IC, Rodrigo MJ, Monteiro Marques JG. Two siblings with periodic fever, aphthous stomatitis, pharyngitis, adenitis (PFAPA) syndrome. *Pediatr Infect Dis J* 2009; 28: 254-5.
- [15] Valenzuela PM, Majerson D, Tapia JL, Talesnik E. Syndrome of periodic fever, aphthous stomatitis, pharyngitis, and adenitis (PFAPA) in siblings. *Clin Rheumatol* 2009; 28: 1235-7.
- [16] Adachi M, Watanabe A, Nishiyama A, *et al.* Familial cases of periodic fever with aphthous stomatitis, pharyngitis, and cervical adenitis syndrome. *J Pediatr* 2011; 158: 155-9.
- [17] Domingo C, Touitou I, Bayou A, *et al.* Familial Mediterranean fever in the 'Chuetas' of Mallorca: a question of Jewish origin or genetic heterogeneity. *Eur J Hum Genet* 2000; 8: 242-6.
- [18] Tsuchiya-Suzuki A, Yazaki M, Nakamura A, *et al.* Clinical and genetic features of familial Mediterranean fever in Japan. *J Rheumatol* 2009; 36: 1671-6.
- [19] Tomiyama N, Higashiesato Y, Oda T, *et al.* *MEFV* mutation analysis of familial Mediterranean fever in Japan. *Clin Exp Rheumatol* 2008; 26: 13-7.
- [20] Tchemitchko D, Legendre M, Cazeneuve C, Delahaye A, Niel F, Amselem S. The *E148Q MEFV* allele is not implicated in the development of familial Mediterranean fever. *Hum Mutat* 2003; 22: 339-40.
- [21] Rabinovich E, Shinar Y, Leiba M, Ehrenfeld M, Langevitz P, Livneh A. Common FMF alleles may predispose to development of Behcet's disease with increased risk for venous thrombosis. *Scand J Rheumatol* 2007; 36: 48-52.
- [22] Uslu N, Yüce A, Demir H, *et al.* The association of inflammatory bowel disease and Mediterranean fever gene (*MEFV*) mutations in Turkish children. *Dig Dis Sci*. 2010; 55: 3488-94.
- [23] Giaglis S, Mimidis K, Papadopoulos V, *et al.* Increased frequency of mutations in the gene responsible for familial Mediterranean fever (*MEFV*) in a cohort of patients with ulcerative colitis: evidence for a potential disease-modifying effect? *Dig Dis Sci* 2006; 51: 687-92.
- [24] Gershoni-Baruch R, Broza Y, Brik R. Prevalence and significance of mutations in the familial Mediterranean fever gene in Henoch-Schönlein purpura. *J Pediatr* 2003; 143: 658-61.
- [25] Özçakar ZB, Yalçinkaya F, Cakar N, *et al.* *MEFV* mutations modify the clinical presentation of Henoch-Schönlein purpura. *J Rheumatol* 2008; 35: 2427-9.
- [26] Rabinovitch E, Harats D, Yaron P, *et al.* Familial Mediterranean fever gene and protection against asthma. *Ann Allergy Asthma Immunol* 2007; 99: 517-21.
- [27] Berkun Y, Levy R, Hurwitz A, *et al.* The familial Mediterranean fever gene as a modifier of periodic fever, aphthous stomatitis, pharyngitis, and adenopathy syndrome. *Semin Arthritis Rheum* 2011; 40: 467-72.

Received: January 22, 2013

Revised: March 9, 2013

Accepted: March 14, 2013

© Taniuchi *et al.*; Licensee Bentham Open.

This is an open access article licensed under the terms of the Creative Commons Attribution Non-Commercial License (<http://creativecommons.org/licenses/by-nc/3.0/>) which permits unrestricted, non-commercial use, distribution and reproduction in any medium, provided the work is properly cited.

# Genetic correction of *HAX1* in induced pluripotent stem cells from a patient with severe congenital neutropenia improves defective granulopoiesis

Tatsuya Morishima,<sup>1</sup> Ken-ichiro Watanabe,<sup>1</sup> Akira Niwa,<sup>2</sup> Hideyo Hirai,<sup>3</sup> Satoshi Saida,<sup>1</sup> Takayuki Tanaka,<sup>2</sup> Itaru Kato,<sup>1</sup> Katsutsugu Umeda,<sup>1</sup> Hidefumi Hiramatsu,<sup>1</sup> Megumu K. Saito,<sup>2</sup> Kousaku Matsubara,<sup>4</sup> Souichi Adachi,<sup>5</sup> Masao Kobayashi,<sup>6</sup> Tatsutoshi Nakahata,<sup>2</sup> and Toshio Heike<sup>1</sup>

<sup>1</sup>Department of Pediatrics, Graduate School of Medicine, Kyoto University, Kyoto; <sup>2</sup>Department of Clinical Application, Center for iPS Cell Research and Application, Kyoto University, Kyoto; <sup>3</sup>Department of Transfusion Medicine and Cell Therapy, Kyoto University Hospital, Kyoto; <sup>4</sup>Department of Pediatrics, Nishi-Kobe Medical Center, Kobe; <sup>5</sup>Human Health Sciences, Graduate School of Medicine, Kyoto University, Kyoto; and <sup>6</sup>Department of Pediatrics, Hiroshima University Graduate School of Biomedical Sciences, Hiroshima, Japan

## ABSTRACT

*HAX1* was identified as the gene responsible for the autosomal recessive type of severe congenital neutropenia. However, the connection between mutations in the *HAX1* gene and defective granulopoiesis in this disease has remained unclear, mainly due to the lack of a useful experimental model for this disease. In this study, we generated induced pluripotent stem cell lines from a patient presenting for severe congenital neutropenia with *HAX1* gene deficiency, and analyzed their *in vitro* neutrophil differentiation potential by using a novel serum- and feeder-free directed differentiation culture system. Cytostaining and flow cytometric analyses of myeloid cells differentiated from patient-derived induced pluripotent stem cells showed arrest at the myeloid progenitor stage and apoptotic predisposition, both of which replicated abnormal granulopoiesis. Moreover, lentiviral transduction of the *HAX1* cDNA into patient-derived induced pluripotent stem cells reversed disease-related abnormal granulopoiesis. This *in vitro* neutrophil differentiation system, which uses patient-derived induced pluripotent stem cells for disease investigation, may serve as a novel experimental model and a platform for high-throughput screening of drugs for various congenital neutrophil disorders in the future.

## Introduction

Severe congenital neutropenia (SCN) is a rare myelopoietic disorder resulting in recurrent life-threatening infections due to a lack of mature neutrophils,<sup>1</sup> and individuals with SCN present for myeloid hypoplasia with an arrest of myelopoiesis at the promyelocyte/myelocyte stage.<sup>1,2</sup> SCN is actually a multigene syndrome that can be caused by inherited mutations in several genes. For instance, approximately 60% of SCN patients are known to carry autosomal dominant mutations in the *ELANE* gene, which encodes neutrophil elastase (NE).<sup>3</sup> An autosomal recessive type of SCN was first described by Kostmann in 1956,<sup>4</sup> and defined as Kostmann disease. Although the gene responsible for this classical type of SCN remained unknown for more than 50 years, Klein *et al.* identified mutations in *HAX1* to be responsible for this type of SCN in 2007.<sup>5</sup> *HAX1* localizes predominantly to mitochondria, where it controls inner mitochondrial membrane potential ( $\Delta\Psi_m$ ) and apoptosis.<sup>6,7</sup> Although an increase in apoptosis in mature neutrophils was presumed to cause neutropenia in *HAX1* gene deficiency,<sup>5</sup> the connection between *HAX1* gene mutations and defective granulopoiesis in SCN has remained unclear.

To control infections, SCN patients are generally treated with granulocyte colony-stimulating factor (G-CSF); howev-

er, long-term G-CSF therapy associates with an increased risk of myelodysplastic syndrome and acute myeloid leukemia (MDS/AML).<sup>8,9</sup> Although hematopoietic stem cell transplantations are available as the only curative therapy for this disease, they can result in various complications and mortality.<sup>4</sup>

Many murine models of human congenital and acquired diseases are invaluable for disease investigation as well as for novel drug discoveries. However, their use in a research setting can be limited if they fail to mimic strictly the phenotype of the human disease in question. For instance, the *Hax1* knock-out mouse is characterized by lymphocyte loss and neuronal apoptosis, but not neutropenia.<sup>10</sup> Thus, it is not a suitable experimental model for SCN. Induced pluripotent stem (iPS) cells are reprogrammed somatic cells with embryonic stem (ES) cell-like characteristics produced by the introduction of specific transcription factors,<sup>11,16</sup> and they may substitute murine models of human disease. It is believed that iPS cell technology, which generates disease-specific pluripotent stem cells in combination with directed cell differentiation, will contribute enormously to patient-oriented research, including disease pathophysiology, drug screening, cell transplantation, and gene therapy.

*In vitro* neutrophil differentiation systems, which can reproduce the differentiation of myeloid progenitor cells to mature neutrophils, are needed to understand the pathogenesis of SCN better. Recently, we established a neutrophil differentia-

©2013 Ferrata Storti Foundation. This is an open-access paper. doi:10.3324/haematol.2013.083873

The online version of this article has a Supplementary Appendix.

Manuscript received on January 9, 2013. Manuscript accepted on August 20, 2013.

Correspondence: heike@kuhp.kyoto-u.ac.jp

tion system from human iPS cells<sup>17</sup> as well as a serum- and feeder-free monolayer hematopoietic culture system from human ES and iPS cells.<sup>18</sup> In this study, we generate iPS cell lines from an SCN patient with *HAX1* gene deficiency and differentiate them into neutrophils *in vitro*. Furthermore, we corrected for the *HAX1* gene deficiency in HAX1-iPS cells by lentiviral transduction with *HAX1* cDNA and analyzed the neutrophil differentiation potential of these cells. Thus, this *in vitro* neutrophil differentiation system from patient-derived iPS cells may be a useful model for future studies in SCN patients with *HAX1* gene deficiency.

## Methods

### Human iPS cell generation

Skin biopsy specimens were obtained from an 11-year old male SCN patient with *HAX1* gene deficiency.<sup>19</sup> This study was approved by the Ethics Committee of Kyoto University, and informed consent was obtained from the patient's guardians in accordance with the Declaration of Helsinki. Fibroblasts were expanded in DMEM (Nacalai Tesque, Inc., Kyoto, Japan) containing 10% FBS (vol/vol, Invitrogen, Carlsbad, CA, USA) and 0.5% penicillin and streptomycin (wt/vol, Invitrogen). Generation of iPS cells was performed as described previously.<sup>12</sup> In brief, we introduced *OCT3/4*, *SOX2*, *KLF4*, and *cMYC* using ecotropic retroviral transduction into patient's fibroblasts expressing mouse *Slc7a1*. Six days after transduction, cells were harvested and re-plated onto mitotically inactive SNL feeder cells. On the following day, DMEM was replaced with primate ES cell medium (ReproCELL, Kanagawa, Japan) supplemented with basic fibroblast growth factor (5 ng/mL, R&D Systems, Minneapolis, MN, USA). Three weeks later, individual colonies were isolated and expanded.

### Maintenance of cells

Control ES (KhES-1) and control iPS (253G4 and 201B6) cells were kindly provided by Drs. Norio Nakatsuji and Shinya Yamanaka (Kyoto University, Kyoto, Japan), respectively. These human ES and iPS cell lines were maintained on mitomycin-C (Kyowa Hakko Kirin, Tokyo, Japan)-treated SNL feeder cells as described previously<sup>17</sup> and subcultured onto new SNL feeder cells every seven days.

### Flow cytometric analysis

Cells were stained with antibodies as reported previously.<sup>17</sup> Samples were analyzed using an LSR flow cytometer and Cell Quest software (Becton-Dickinson).

### Neutrophil differentiation of iPS cells

In a previous study, we established a serum and feeder-free monolayer hematopoietic culture system from human ES and iPS cells.<sup>18</sup> In this study, we modified this culture system to direct neutrophil differentiation. iPS cell colonies were cultured on growth factor-reduced Matrigel (Becton-Dickinson)-coated cell culture dishes in Stemline II hematopoietic stem cell expansion medium (Sigma-Aldrich, St. Louis, MO, USA) containing the insulin-transferrin-selenium (ITS) supplement (Invitrogen) and cytokines. iPS cells were treated with cytokines as follows: bone morphogenetic protein (BMP) 4 (20 ng/mL, R&D Systems) was added for four days and then replaced with vascular endothelial growth factor (VEGF) 165 (40 ng/mL, R&D Systems) on Day 4. On Day 6, VEGF 165 was replaced with a combination of stem cell factor (SCF, 50 ng/mL, R&D Systems), interleukin (IL)-3 (50 ng/mL, R&D Systems), thrombopoietin (TPO, 5 ng/mL, kindly provided by

Kyowa Hakko Kirin), and G-CSF (50 ng/mL, also kindly provided by Kyowa Hakko Kirin). Thereafter, medium was replaced every five days.

### Dead cell removal and CD45<sup>+</sup> leukocyte separation

Floating cells were collected, followed by the removal of dead cells and cellular debris with the Dead Cell Removal kit (Miltenyi Biotec, Bergisch Gladbach, Germany). CD45<sup>+</sup> cells were then separated using human CD45 microbeads (Miltenyi Biotec). Cell separation procedures were performed using the autoMACS Pro Separator (Miltenyi Biotec).

### Statistical analysis

Statistical analysis was carried out using Student's t-test.  $P < 0.05$  was considered statistically significant.

## Results

### Generation of iPS cell lines from an SCN patient with *HAX1* gene deficiency

To generate patient-derived iPS cell lines, dermal fibroblasts were obtained from a male SCN patient with a homozygous 256C-to-T transition resulting in an R86X mutation in the *HAX1* gene.<sup>19</sup> These fibroblasts were reprogrammed to iPS cells after transduction with retroviral vectors encoding *OCT3/4*, *SOX2*, *KLF4* and *cMYC*,<sup>12</sup> and a total of 11 iPS cell clones were obtained. From these, we randomly selected three clones for propagation and subsequent analyses. One of these clones (HAX1 4F5) was generated with four factors (*OCT3/4*, *SOX2*, *KLF4*, and *cMYC*); the remaining clones (HAX1 3F3 and 3F5) were reprogrammed with three factors (*OCT3/4*, *SOX2*, and *KLF4*).<sup>12</sup>

All of these patient-derived iPS cell clones showed a characteristic human ES cell-like morphology (Figure 1A), and they propagated for serial passages in human ES cell maintenance culture medium. Quantitative PCR analysis showed the expression of *NANOG*, a pluripotent marker gene, to be comparable to that of control ES (KhES-1) and iPS (253G4 and 201B6) cells (Figure 1B). Surface marker analysis indicated that they were also positive for SSEA4, a human ES and iPS cell marker (Figure 1C). DNA sequencing analysis verified an identical mutation in the *HAX1* gene in all established iPS cell clones (Figure 1D). The pluripotency of all iPS cell clones was confirmed by the presence of cell derivatives representing all three germ layers by teratoma formation after subcutaneous injection of undifferentiated iPS cells into immunocompromised NOD/SCID/ $\gamma$ c<sup>null</sup> mice (Figure 1E).

To validate the authenticity of iPS cells further, we investigated the expression of the four genes that were used for iPS cell generation. The expression level of all endogenous genes was comparable to control ES and iPS cells. On the other hand, transgene expression was largely undetectable in patient-derived iPS cell clones (Online Supplementary Figure S1A). Chromosomal analysis revealed that all patient-derived iPS cell clones maintained a normal karyotype (Online Supplementary Figure S1B). Genetic identity was shown by short tandem repeat analysis (Online Supplementary Figure S1C).

Taken collectively, these results indicate that iPS cell clones were comprised of good quality iPS cells derived from the somatic cells of an SCN patient with *HAX1* gene deficiency (HAX1-iPS cells).

### Maturation arrest at the progenitor level in neutrophil differentiation from *HAX1*-iPS cells

The paucity of mature neutrophils in the peripheral blood and a maturation arrest at the promyelocyte/myelocyte stage in the bone marrow are characteristic laboratory findings presented in the SCN patients with *HAX1* gene deficiency. To investigate whether our patient-derived iPS cell model accurately replicated this disease phenotype, we assessed neutrophil differentiation from *HAX1*-iPS cells by using a serum- and feeder-free monolayer culture system<sup>18</sup> with minor modifications (Online Supplementary Figure S2).

In this system, we cultured iPS cell colonies on Matrigel-coated dishes in serum-free medium supplemented with several cytokines and obtained hematopoietic cells as floating cells on approximately Day 26 of differentiation. May-Giemsa staining of floating live CD45<sup>+</sup> cells derived from normal iPS cells showed that approximately 40% were mature neutrophils (Figure 2A and B). The remaining cells consisted of immature myeloid cells as well as a small number of macrophages. Cells of other lineages such as erythroid or lymphoid cells were not observed. On the other hand, *HAX1*-iPS cell-derived blood cells contained only approximately 10% mature neutrophils and approxi-

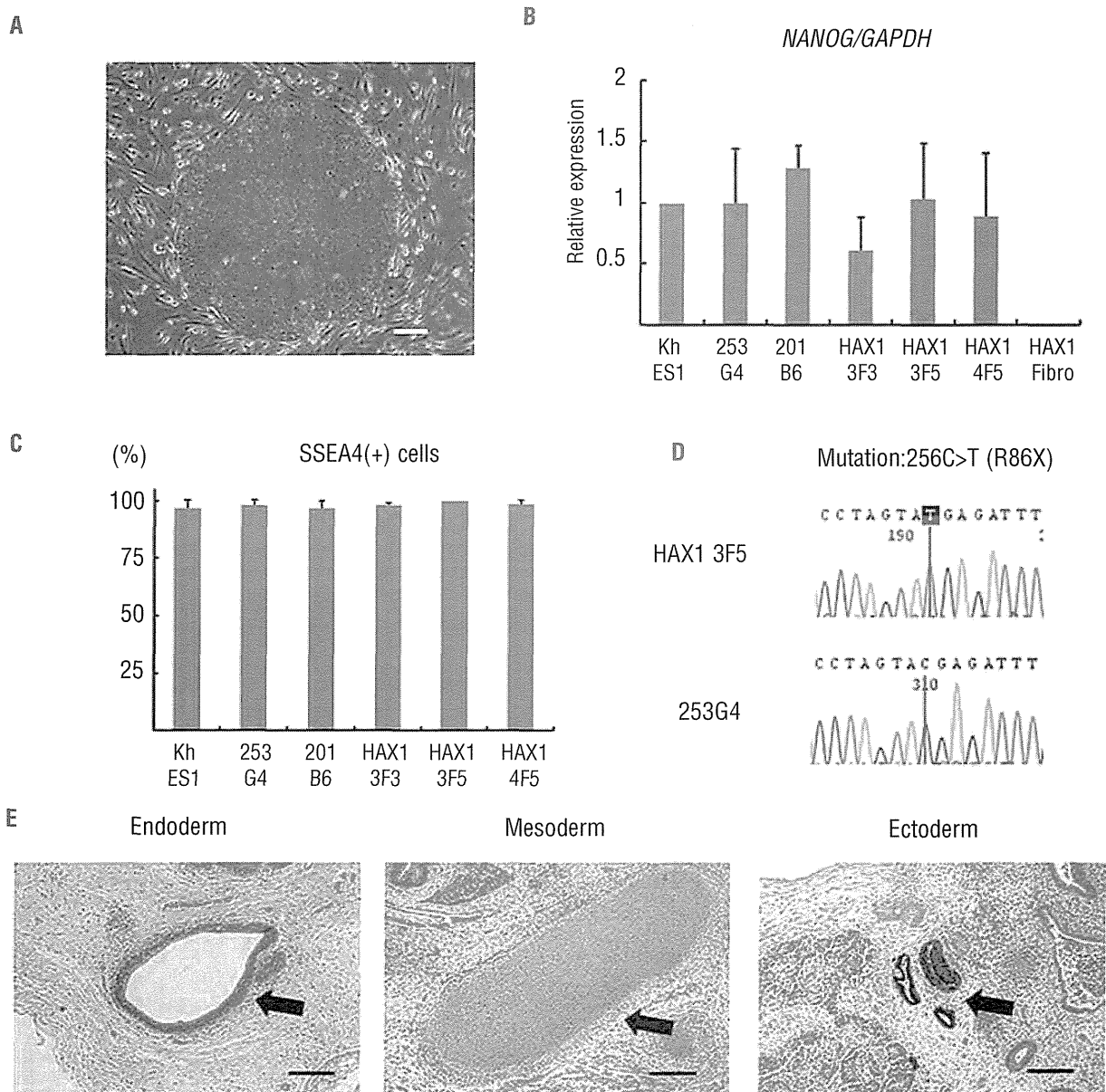
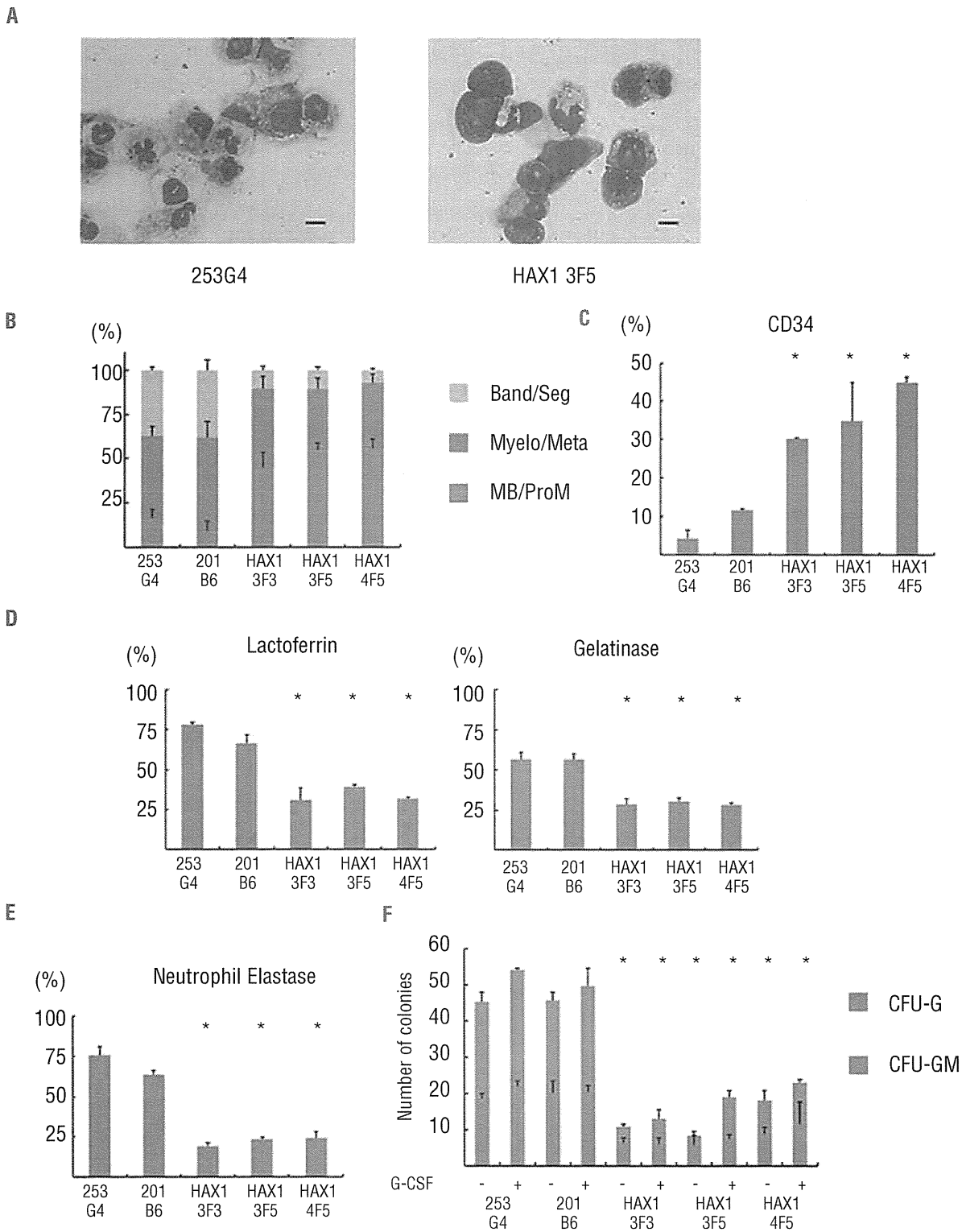


Figure 1. Generation of iPS cell lines from an SCN patient with *HAX1* gene deficiency. (A) Human ES cell-like morphology of *HAX1*-iPS cells. Scale bar: 200  $\mu$ m. (B) *NANOG* expression in *HAX1*-iPS cells, control iPS cells (253G4 and 201B6), and patient-derived fibroblasts (*HAX1* Fibro) compared to control ES cells (KhES1). *GAPDH* was used as an internal control (n = 3; bars represent SDs). (C) SSEA-4 expression analysis using flow cytometry. Gated on TRA1-85<sup>+</sup>DAPI<sup>+</sup> cells as viable human iPS (ES) cells (n = 3; bars represent SDs). (D) DNA sequencing analysis of the *HAX1* gene in iPS cells. *HAX1*-iPS cells showed 256C>T (R86X) mutation that was found in the patient. (E) Teratoma formation from *HAX1*-iPS cells in the NOD/SCID/ $\gamma$ c<sup>null</sup> (NOG) mouse. Arrows indicate the following; Endoderm: respiratory epithelium; Mesoderm: cartilage; Ectoderm: pigmented epithelium. Scale bars: 200  $\mu$ m. (A, D-E) Representative data (*HAX1* 3F5) are shown.



**Figure 2. Maturation arrest at the progenitor level in neutrophil differentiation from HAX1-iPS cells.** (A) May-Giemsa staining of CD45<sup>+</sup> cells derived from normal (253G4) and HAX1-iPS (HAX1 3F5) cells. Scale bars: 10  $\mu$ m. (B) Morphological classification of CD45<sup>+</sup> cells derived from iPS cells. Cells were classified into three groups: myeloblast and promyelocyte (MB/ProM), myelocyte and metamyelocyte (Myelo/Meta), and band and segmented neutrophils (Band/Seg) (n = 3; bars represent SDs). (C) Flow cytometric analysis of CD45<sup>+</sup> cells derived from iPS cells. Cells gated on human CD45<sup>+</sup> DAPI were analyzed (n = 3; bars represent SDs; \*P<0.05 compared to control iPS cells). (D) Immunocytochemical analysis of CD45<sup>+</sup> cells derived from iPS cells (n = 3; bars represent SDs; \*P<0.05 compared to control iPS cells). (E) NE staining of CD45<sup>+</sup> cells derived from iPS cells (n = 3; bars represent SDs; \*P<0.05 compared to control iPS cells). (F) Colony-forming assay of cells derived from iPS cells. On Day 16, living adherent cells were collected and cultured in methylcellulose medium (see *Online Supplementary Appendix*). The number of colonies generated from 1 $\times$ 10<sup>4</sup> cells is indicated (n = 3; bars represent SD; \*P<0.05 compared to control iPS cells). (A–E) Live CD45<sup>+</sup> cells derived from normal and HAX1-iPS cells on Day 26 of neutrophil differentiation were analyzed. Dead cells and CD45<sup>+</sup> cells were depleted using an autoMACS Pro separator (see *Methods*).

mately 50% immature myeloid cells, including myeloblasts and promyelocytes (Figure 2A and B). Flow cytometric analysis revealed that the percentage of CD34<sup>+</sup> cells within HAX1-iPS cell-derived blood cells was significantly higher than in normal iPS cell-derived blood cells (Figure 2C), which also showed that the percentage of phenotypically immature myeloid cells was higher in HAX1-iPS cell-derived blood cells than in normal iPS cell-derived blood cells.

Immunocytochemical analysis for lactoferrin and gelatinase, which are constitutive proteins of neutrophil specific granules observed in mature neutrophils, showed that the proportion of these granule-positive cells was significantly lower in HAX1-iPS cell-derived blood cells than in normal iPS cell-derived blood cells (Figure 2D). NE is a protease stored in primary granules of neutrophilic granulocytes that are formed at the promyelocytic phase of granulocyte differentiation. *ELANE* mRNA expression in myeloid progenitors and the protein level of NE in plasma are markedly reduced in SCN patients with mutations in *ELANE* or *HAX1*.<sup>20</sup> Consistent with this, the proportion of NE-positive cells was significantly lower in blood cells derived from HAX1-iPS cells than in those derived from normal iPS cells (Figure 2E). Thus, the level of functionally mature neutrophils decreased during *in vitro* granulopoietic differentiation of HAX1-iPS cells.

Next, we analyzed the colony-forming potential of HAX1-iPS cell-derived myeloprogenitor cells. Significantly fewer colonies, which were classified as granulocyte-macrophage (GM) or granulocyte (G) colony-forming units (CFU), were derived from HAX1-iPS cells than from control iPS cells. Furthermore, the colonies derived from HAX1-iPS cells were predominantly CFU-GM (Figure 2F). Thus, maturation arrest occurred at the clonogenic progenitor stage during *in vitro* neutrophil differentiation of HAX1-iPS cells.

SCN is characterized by severe neutropenia with very low absolute neutrophil counts in peripheral blood, and many SCN patients respond to G-CSF treatment.<sup>1,2</sup> In colony-forming assays using bone marrow cells of SCN patients, primitive myeloid progenitor cells have reduced responsiveness to hematopoietic cytokines including G-CSF.<sup>21,22</sup> Therefore, we next examined the response of HAX1-iPS cell-derived blood cells to G-CSF using a colony-forming assay. Although the number of colonies

derived from HAX1-iPS cells slightly increased following the addition of G-CSF, it remained significantly lower than the number of colonies derived from control iPS cells in the absence of G-CSF (Figure 2F). These results indicate that the responsiveness of HAX1-iPS-derived blood cells to G-CSF was insufficient to restore the neutrophil count to a normal level and are consistent with the fact that the absolute neutrophil counts of SCN patients remain low following G-CSF therapy.<sup>19,21</sup>

#### Neutrophils derived from HAX1-iPS cells are predisposed to undergo apoptosis due to their reduced $\Delta\psi_m$

Previous studies have shown HAX1 to localize to mitochondria<sup>6</sup> and to mediate anti-apoptotic activity.<sup>7</sup> Interestingly, this apoptotic predisposition of neutrophils due to their reduced  $\Delta\psi_m$  was observed in HAX1-deficient patients,<sup>5</sup> prompting us to examine apoptosis in HAX1-iPS cell-derived blood cells. Consistent with these reports, HAX1-iPS cell-derived blood cells showed a significantly higher percentage of Annexin V-positive cells than in control cells (Figure 3A). In addition, a mitochondrial membrane potential assay revealed that the percentage of cells with a low  $\Delta\psi_m$  was significantly higher in HAX1-iPS cell-derived blood cells than in blood cells derived from control iPS cells (Figure 3B). By contrast, the percentage of cells with a low  $\Delta\psi_m$  was similar in undifferentiated HAX1-iPS cells and undifferentiated control iPS cells (Online Supplementary Figure S3).

Thus, increased apoptosis due to reduced  $\Delta\psi_m$  causes defective granulopoiesis during neutrophil differentiation from HAX1-iPS cells, similar to the process observed in SCN patients with *HAX1* gene deficiency.

#### Lentiviral transduction of HAX1 cDNA improves maturation arrest and apoptotic predisposition of HAX1-iPS cells

Because most *HAX1* gene mutations in SCN patients are nonsense mutations resulting in a premature stop codon and protein truncation,<sup>23</sup> loss of the HAX1 protein is believed to cause severe neutropenia. To uncover the pathophysiological hallmarks of this disease, we performed lentiviral transduction of *HAX1* cDNA into HAX1-iPS cells.

We constructed lentiviral vectors that expressed *HAX1* cDNA and EGFP as a marker gene (pCSII-EF-IEGFP; EGFP

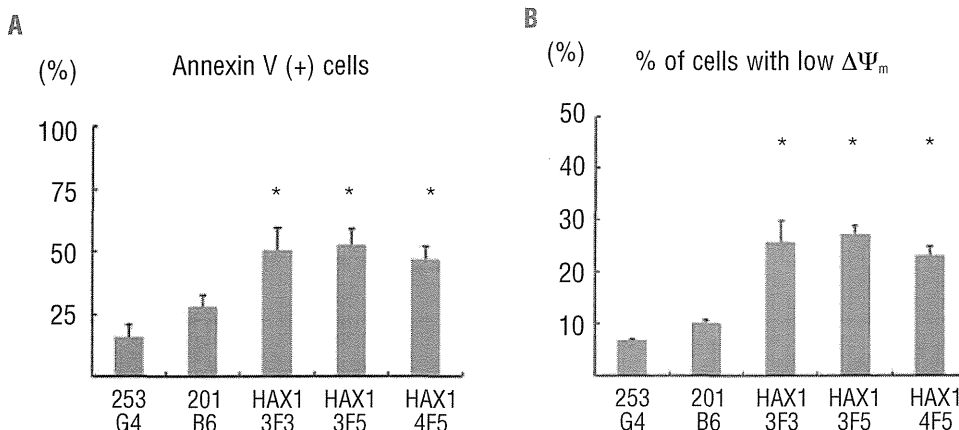


Figure 3. Neutrophils derived from HAX1-iPS cells are predisposed to undergo apoptosis due to their reduced  $\Delta\psi_m$ . Annexin V assay (A) and mitochondrial membrane potential assay (B) of iPS cell-derived cells on Day 26 of neutrophil differentiation using flow cytometry. Cells gated on human CD45<sup>+</sup> were analyzed (n = 3; bars represent SDs; \* $P < 0.05$  to control iPS cells).

only, pCSII-EF-HAX1-IEGFP; HAX1 cDNA and EGFP) (Figure 4A). Efficient transduction of HAX1-iPS cells with these lentiviral vectors (HAX1 3F5+GFP; HAX1 3F5 transduced with pCSII-EF-IEGFP, HAX1 3F5+HAX1; HAX1 3F5 transduced with pCSII-EF-HAX1-IEGFP) was confirmed by a significant increase in HAX1 protein by Western blotting analysis (Figure 4B).

We then differentiated these lentiviral-transduced iPS cells into neutrophils, and examined whether defective granulopoiesis and apoptotic predisposition could be reversed. Morphologically, cells derived from HAX1 3F5+HAX1 showed a higher proportion of mature neutrophils than cells derived from HAX1 3F5+GFP and HAX1 3F5 (Figure 5A and B). Flow cytometric analysis revealed that the proportion of CD34<sup>+</sup> cells was significantly lower in the cells derived from HAX1 3F5+HAX1 than HAX1 3F5+GFP and HAX1 3F5 (Figure 5C). Immunocytochemical analysis for lactoferrin and gelatinase showed that the proportion of these granule-positive cells in generated blood cells was significantly higher in HAX 3F5+HAX1 than in HAX13F5+GFP and HAX1 3F5 (Figure 5D). These results indicated that *HAX1* cDNA increased the number of mature neutrophils in the neutrophil differentiation culture from HAX1-iPS cells *in vitro*. In addition, the percentage of NE-positive cells was significantly higher in cells derived from HAX1 3F5+HAX1 than in cells derived from HAX1 3F5+GFP and HAX1 3F5 (Figure 5E). Furthermore, the number of colonies derived from HAX1 3F5+HAX1 was comparable to the number derived from control cells (Figure 5F).

HAX1 3F5+HAX1-derived blood cells showed a significantly lower percentage of Annexin V-positive cells (Figure 6A) and a significantly lower percentage of cells with a low  $\Delta\psi_m$  (Figure 6B) than HAX13F5+GFP and HAX1 3F5-derived blood cells. These results indicated that only *HAX1* cDNA transduction improved defective granulopoiesis and apoptotic predisposition due to low  $\Delta\psi_m$  in the neutrophil differentiation culture from HAX1-iPS cells *in vitro*.

## Discussion

Animal models and *in vitro* cultures consisting of cells derived from patients are often used to investigate disease pathophysiology and to develop novel therapies. Unfortunately, *Hax1* knock-out mice fail to reproduce abnormal granulopoiesis as observed in SCN patients.<sup>10</sup> Moreover, bone marrow cells are not an ideal experimental tool because it is difficult to obtain sufficient blood cells due to the invasiveness of the aspiration procedure. Moreover, the pathophysiological mechanisms occurring during early granulopoiesis are difficult to address in primary patient samples.

Our established culture system efficiently induced directed hematopoietic differentiation, which consisted of myeloid cells at different stages of development, from various control and patient-derived HAX1-iPS cell lines. Furthermore, this *in vitro* neutrophil differentiation system produced sufficient myeloid cells, which enabled us to perform various types of assays. In addition, flow cytom-

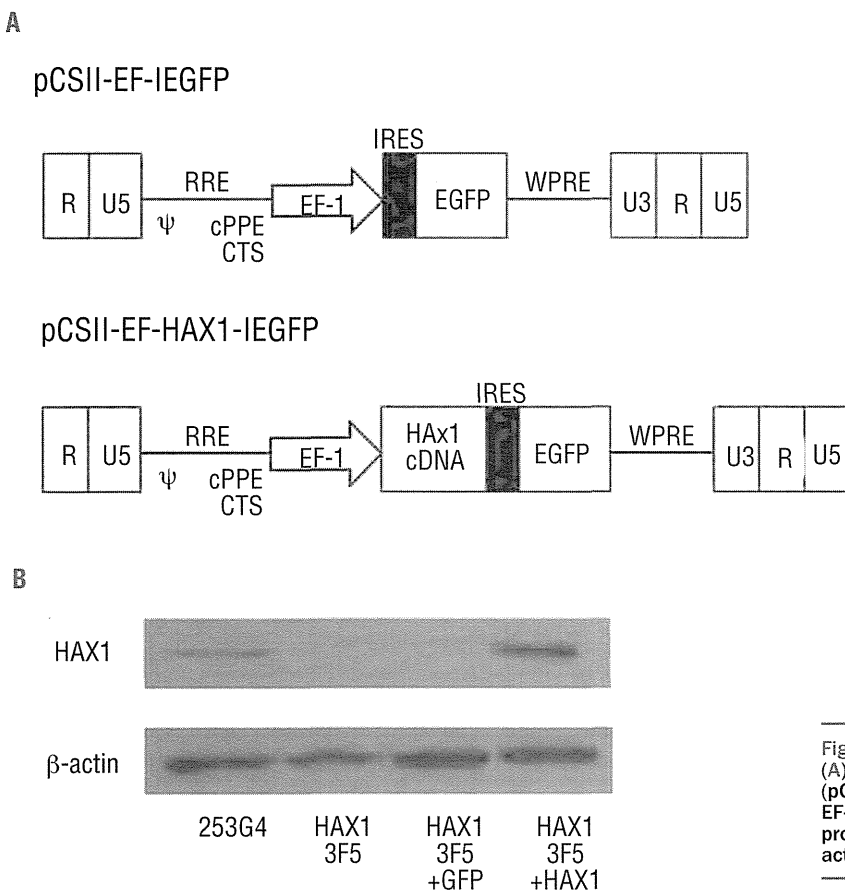


Figure 4. Lentiviral transduction of HAX1-iPS cells. (A) Lentiviral vector constructs with only EGFP (pCSII-EF-IEGFP), and *HAX1* cDNA and EGFP (pCSII-EF-HAX1-IEGFP). (B) Western blot analysis for HAX1 protein in lentivirally-transduced HAX1-iPS cells.  $\beta$ -actin was used as a loading control.



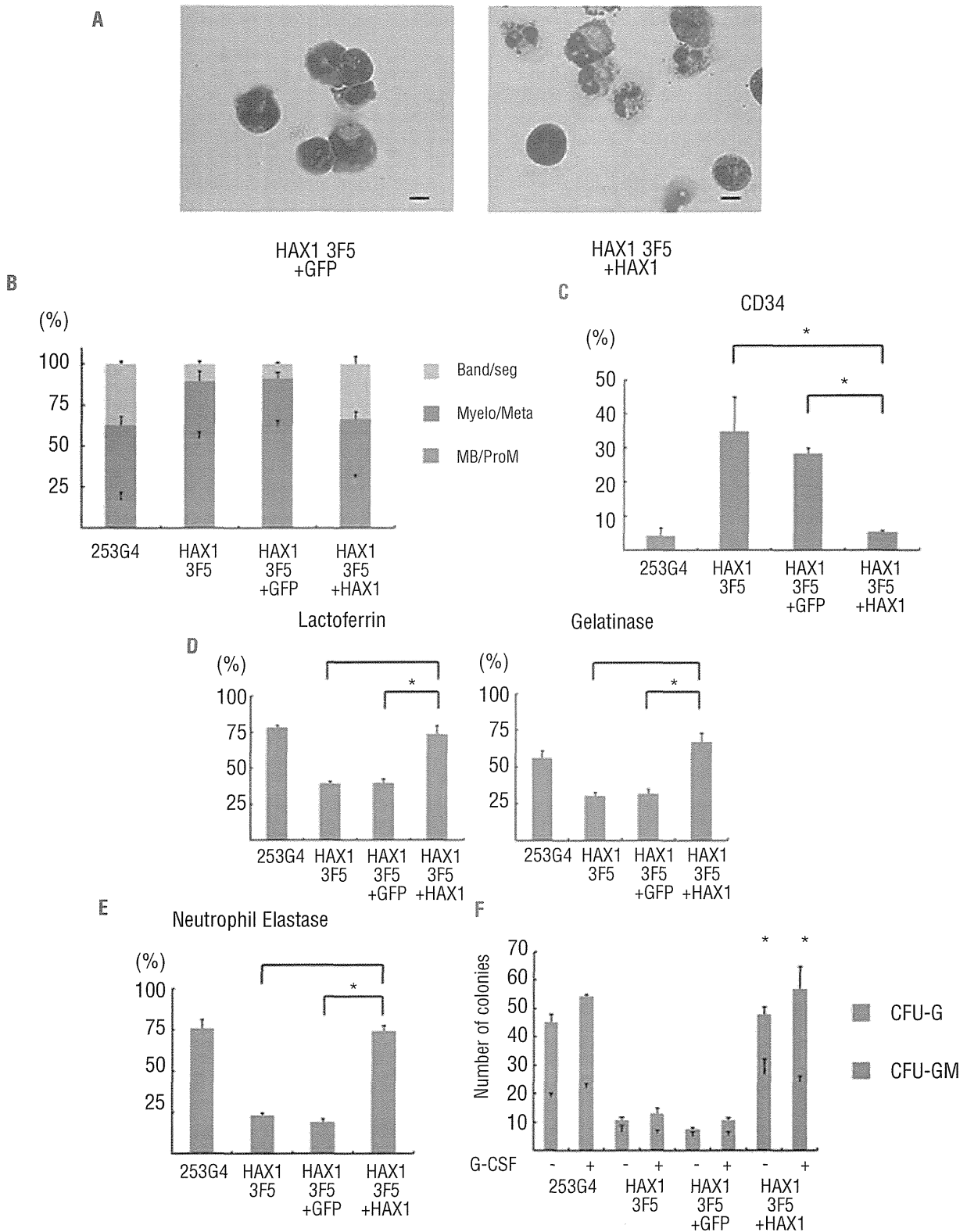


Figure 5. Lentiviral transduction of HAX1 cDNA improves maturation arrest of HAX1-iPS cells. (A) May-Giemsa staining of CD45<sup>+</sup> cells derived from HAX1 3F5+GFP and HAX1 3F5+HAX1 cells. Scale bars: 10  $\mu$ m. (B) Morphological classification of CD45<sup>+</sup> cells derived from lentivirally-transduced iPS cells. (n = 3; bars represent SDs). (C) Flow cytometric analysis of CD45<sup>+</sup> cells derived from lentivirally-transduced iPS cells. Cells gated on GFP<sup>+</sup> human CD45<sup>+</sup> DAPI were analyzed (n = 3; bars represent SDs; \*P<0.05). (D) Immunocytochemical analysis of CD45<sup>+</sup> cells derived from lentivirally-transduced iPS cells (n = 3; bars represent SDs; \*P<0.05). (E) NE staining of CD45<sup>+</sup> cells derived from lentivirally-transduced iPS cells (n = 3; bars represent SDs; \*P<0.05). (F) Colony-forming assay of lentivirally-transduced cells derived from iPS cells. The number of colonies derived from 1 $\times$ 10<sup>4</sup> cells is indicated (n = 3; bars represent SD; \*P<0.05 compared to HAX1 3F5 and HAX1 3F5+GFP). (A-E) Live CD45<sup>+</sup> cells derived from lentivirally-transduced iPS cells on Day 26 of neutrophil differentiation were analyzed. Dead cells and CD45<sup>-</sup> cells were depleted using an autoMACS Pro separator (see *Methods*).

etry, a colony-forming assay, and cytochemical staining of HAX1-iPS cell-derived blood cells quantitatively demonstrated maturation arrest at the progenitor level and apoptotic predisposition due to low  $\Delta\Psi_m$ , resulting in defective granulopoiesis, which were typically observed in SCN patients with *HAX1* gene deficiency. Thus, our culture system may serve as a novel experimental model and a platform for high-throughput screening of drugs for neutropenia in SCN with *HAX1* gene deficiency.

A colony-forming assay showed that the response to G-CSF administration correlated well with the responsiveness of SCN patients to G-CSF therapy. Defective granulopoiesis was recently reported in SCN-iPS cells with a mutation in *ELANE*.<sup>24</sup> Our data showing defective granulopoiesis and reduced response to G-CSF administration are generally consistent with this report. The slight differences in CFU-G/GM colony-forming potential between this previous study and the current study might be due to differences in the causative gene (*HAX1* or *ELANE*) or the culture system used for neutrophil differentiation, and/or to variation in the differentiation capabilities of the clones.

In our serum and feeder-free monolayer culture system, human ES and iPS cells differentiate into hematopoietic and endothelial cells via common KDR<sup>+</sup>CD34<sup>+</sup> hemoangiogenic progenitors, which exist during early embryogenesis.<sup>18</sup> Therefore, emergence of abnormal granulopoiesis in this system suggests that disease onset might occur at early hematopoietic stage (yolk sac or fetal liver), which would have never been addressed with patient samples.

We also showed that *HAX1* cDNA transduction could reverse disease-related phenotypes such as abnormal granulopoiesis and apoptotic predisposition. Although little is known about the pathophysiology of SCN with *HAX1* gene deficiency, these results clearly indicated that a loss in HAX1 protein might be the primary cause of neutropenia. These results also indicated the possibility of using patient-derived iPS cells for gene therapy; however, there are technical difficulties that would preclude these cells from being used in a clinical setting. Lentiviral vectors that randomly integrate transgenes can affect the expression of related genes, including cancer-related genes.<sup>25-28</sup> To overcome these problems, we are required to select clones in which transgenes are integrated 'safe harbor' sites and

highly expressed without perturbation of neighboring gene expression,<sup>29</sup> or to take the zinc finger nuclease-mediated gene targeting approach<sup>30-32</sup> specifically to a pre-designed safe harbor site such as the *AAVS1* locus,<sup>33</sup> which has previously been shown to permit stable expression of transgenes with minimal effects on nearby genes.

The pluripotency of patient-derived iPS cells enables investigation of the pathophysiology of various organ abnormalities and/or dysfunctions. Many types of inherited bone marrow failure syndrome were characterized by multisystem developmental defects that affected the heart, kidney, skeletomuscular system, and central nervous system. Among these, neurological symptoms were frequently seen in SCN patients with *HAX1* gene deficiency,<sup>19,23,34</sup> suggesting that a loss in HAX1 may also affect neural development. Indeed, our patient also presented for epilepsy and severe delays in motor, cognitive, and intellectual development.<sup>19</sup> In patient-derived cells,  $\Delta\Psi_m$  was not reduced in undifferentiated iPS cells but was reduced in differentiated neutrophils. No marked abnormalities in teratoma formation by HAX1-iPS cells were observed. These results are partially consistent with the fact that SCN patients with a *HAX1* gene deficiency have only neutropenia and neurological symptoms, despite *HAX1* being a ubiquitously expressed gene.<sup>6</sup> Because some of these neurological symptoms cannot be reproduced in the currently available mouse model,<sup>10</sup> additional studies will be necessary to address the effects of *HAX1* on neural development by directed culture models of patient-derived iPS cells.

In conclusion, patient-derived iPS cell-derived myeloid cells were similar in disease presentation to SCN patients with *HAX1* gene deficiency, which could be reversed by gene correction in a novel *in vitro* neutrophil differentiation system. This culture system will serve as a new tool to facilitate disease modeling and drug screening for congenital neutrophil disorders.

#### Acknowledgments

The authors would like to thank Dr. Norio Nakatsuji for providing the human ES cell line KhES-1, Dr. Shinya Yamanaka for providing human iPS cell lines 201B6 and 253G4, and Dr. Hiroyuki Miyoshi for providing pCSII-EF-MCS. We are grate-

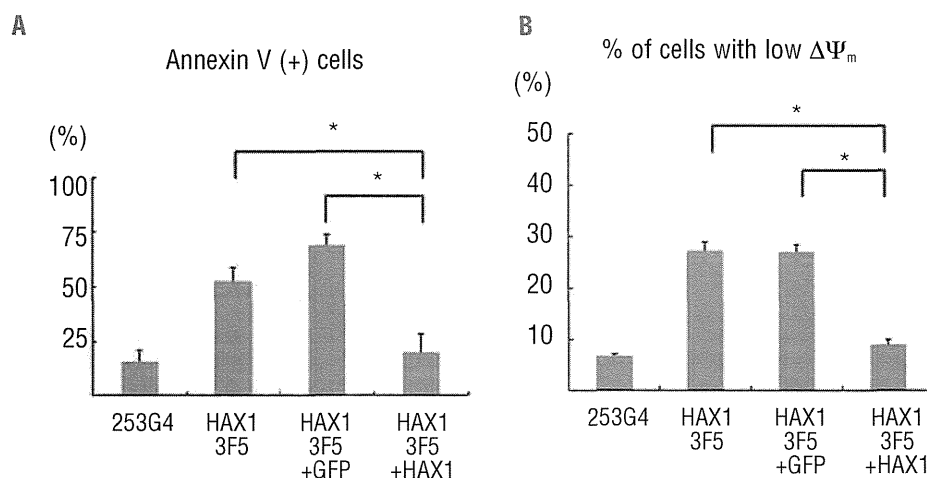


Figure 6. Lentiviral transduction of *HAX1* cDNA prevents *HAX1*-iPS cells being predisposed to undergo apoptosis. Annexin V assay (A) and mitochondrial membrane potential assay (B) of lentivirally-transduced iPS cell-derived cells on Day 26 of neutrophil differentiation. Cells gated on GFP<sup>+</sup> human CD45<sup>+</sup> were analyzed (n = 3; bars represent SDs; \*P < 0.05).

ful to Kyowa Hakko Kirin for providing TPO and G-CSF. We also thank the Center for Anatomical Studies, Kyoto University Graduate School of Medicine, for immunocytochemical analysis. Funding was provided by grants from the Ministry of Health, Labour and Welfare to KW, TN, and TH, a grant from the Ministry of Education, Culture, Sports, Science and Technology (MEXT) to KW, TN, and TH, grants from the Leading Project of MEXT to TN, a grant from Funding Program for World-Leading Innovative Research and Development on Science and Technology (FIRST Program) of Japan Society for the Promotion

of Science (JSPS) to TN, grants from the SENSHIN Medical Research Foundation to IK, and grants from the Fujiwara Memorial Foundation to TM. This work was also supported by the Global COE Program "Center for Frontier Medicine" from MEXT, Japan.

#### Authorship and Disclosures

Information on authorship, contributions, and financial & other disclosures was provided by the authors and is available with the online version of this article at [www.haematologica.org](http://www.haematologica.org).

#### References

1. Welte K, Zeidler C, Dale DC. Severe congenital neutropenia. *Semin Hematol*. 2006;43(3):189-95.
2. Skokowa J, Germeshausen M, Zeidler C, Welte K. Severe congenital neutropenia: inheritance and pathophysiology. *Curr Opin Hematol*. 2007;14(1):22-8.
3. Dale DC, Person RE, Bolyard AA, Aprikyan AG, Bos C, Bonilla MA, et al. Mutations in the gene encoding neutrophil elastase in congenital and cyclic neutropenia. *Blood*. 2000;96(7):2317-22.
4. Kostmann R. Infantile genetic agranulocytosis; agranulocytosis infantilis hereditaria. *Acta Paediatr Suppl*. 1956;45(Suppl 105):1-78.
5. Klein C, Grudzien M, Appaswamy G, Germeshausen M, Sandrock I, Schaffer AA, et al. HAX1 deficiency causes autosomal recessive severe congenital neutropenia (Kostmann disease). *Nat Genet*. 2007;39(1):86-92.
6. Suzuki Y, Demoliere C, Kitamura D, Takeshita H, Deuschle U, Watanabe T. HAX-1, a novel intracellular protein, localized on mitochondria, directly associates with HSI1, a substrate of Src family tyrosine kinases. *J Immunol*. 1997;158(6):2736-44.
7. Sharp TV, Wang HW, Koumi A, Hollyman D, Endo Y, Ye H, et al. K15 protein of Kaposi's sarcoma-associated herpesvirus is latently expressed and binds to HAX-1, a protein with antiapoptotic function. *J Virol*. 2002;76(2):802-16.
8. Freedman MH, Bonilla MA, Fier C, Bolyard AA, Scarlata D, Boxer LA, et al. Myelodysplasia syndrome and acute myeloid leukemia in patients with congenital neutropenia receiving G-CSF therapy. *Blood*. 2000;96(2):429-36.
9. Rosenberg PS, Zeidler C, Bolyard AA, Alter BP, Bonilla MA, Boxer LA, et al. Stable long-term risk of leukaemia in patients with severe congenital neutropenia maintained on G-CSF therapy. *Br J Haematol*. 2010;150(2):196-9.
10. Chao JR, Parganas E, Boyd K, Hong CY, Opferman JT, Ihle JN. Hax1-mediated processing of Htra2 by Parl allows survival of lymphocytes and neurons. *Nature*. 2008;452(7183):98-102.
11. Takahashi K, Yamanaka S. Induction of pluripotent stem cells from mouse embryonic and adult fibroblast cultures by defined factors. *Cell*. 2006;126(4):663-76.
12. Takahashi K, Tanabe K, Ohnuki M, Narita M, Ichisaka T, Tomoda K, et al. Induction of pluripotent stem cells from adult human fibroblasts by defined factors. *Cell*. 2007;131(5):861-72.
13. Meissner A, Wernig M, Jaenisch R. Direct reprogramming of genetically unmodified fibroblasts into pluripotent stem cells. *Nat Biotechnol*. 2007;25(10):1177-81.
14. Okita K, Ichisaka T, Yamanaka S. Generation of germline-competent induced pluripotent stem cells. *Nature*. 2007;448(7151):313-7.
15. Park IH, Zhao R, West JA, Yabuuchi A, Huo H, Ince TA, et al. Reprogramming of human somatic cells to pluripotency with defined factors. *Nature*. 2008;451(7175):141-6.
16. Yu J, Vodyanik MA, Smuga-Otto K, Antosiewicz-Bourget J, Frane JL, Tian S, et al. Induced pluripotent stem cell lines derived from human somatic cells. *Science*. 2007;318(5858):1917-20.
17. Morishima T, Watanabe K, Niwa A, Fujino H, Matsubara H, Adachi S, et al. Neutrophil differentiation from human-induced pluripotent stem cells. *J Cell Physiol*. 2011;226(5):1283-91.
18. Niwa A, Heike T, Umeda K, Oshima K, Kato I, Sakai H, et al. A novel serum-free monolayer culture for orderly hematopoietic differentiation of human pluripotent cells via mesodermal progenitors. *PLoS One*. 2011;6(7):e22261.
19. Matsubara K, Imai K, Okada S, Miki M, Ishikawa N, Tsumura M, et al. Severe developmental delay and epilepsy in a Japanese patient with severe congenital neutropenia due to HAX1 deficiency. *Haematologica*. 2007;92(12):e123-5.
20. Skokowa J, Fobiwé JP, Dan L, Thakur BK, Welte K. Neutrophil elastase is severely down-regulated in severe congenital neutropenia independent of ELA2 or HAX1 mutations but dependent on LEF-1. *Blood*. 2009;114(14):3044-51.
21. Kobayashi M, Yumiba C, Kawaguchi Y, Tanaka Y, Ueda K, Komazawa Y, et al. Abnormal responses of myeloid progenitor cells to recombinant human colony-stimulating factors in congenital neutropenia. *Blood*. 1990;75(11):2143-9.
22. Konishi N, Kobayashi M, Miyagawa S, Sato T, Katoh O, Ueda K. Defective proliferation of primitive myeloid progenitor cells in patients with severe congenital neutropenia. *Blood*. 1999;94(12):4077-83.
23. Germeshausen M, Grudzien M, Zeidler C, Abdollahpour H, Yetgin S, Rezaei N, et al. Novel HAX1 mutations in patients with severe congenital neutropenia reveal isoform-dependent genotype-phenotype associations. *Blood*. 2008;111(10):4954-7.
24. Hiramoto T, Ebihara Y, Mizoguchi Y, Nakamura K, Yamaguchi K, Ueno K, et al. Wnt3a stimulates maturation of impaired neutrophils developed from severe congenital neutropenia patient-derived pluripotent stem cells. *Proc Natl Acad Sci USA*. 2013;110(8):3023-8.
25. Hacein-Bey-Abina S, Von Kalle C, Schmidt M, McCormack MP, Wulffraat N, Leboulch P, et al. LMO2-associated clonal T cell proliferation in two patients after gene therapy for SCID-X1. *Science*. 2003;302(5644):415-9.
26. Ott MG, Schmidt M, Schwarzwaelder K, Stein S, Siler U, Koehl U, et al. Correction of X-linked chronic granulomatous disease by gene therapy, augmented by insertional activation of MDS1-EVI1, PRDM16 or SETBP1. *Nat Med*. 2006;12(4):401-9.
27. Howe SJ, Mansour MR, Schwarzwaelder K, Bartholomae C, Hubank M, Kempinski H, et al. Insertional mutagenesis combined with acquired somatic mutations causes leukemogenesis following gene therapy of SCID-X1 patients. *J Clin Invest*. 2008;118(9):3143-50.
28. Cavazzana-Calvo M, Payen E, Negre O, Wang G, Hehir K, Fusil F, et al. Transfusion independence and HMGA2 activation after gene therapy of human beta-thalassaemia. *Nature*. 2010;467(7313):318-22.
29. Papapetrou EP, Lee G, Malani N, Setty M, Riviere I, Tirunagari LM, et al. Genomic safe harbors permit high beta-globin transgene expression in thalassemia induced pluripotent stem cells. *Nat Biotechnol*. 2011;29(1):73-8.
30. Zou J, Sweeney CL, Chou BK, Choi U, Pan J, Wang H, et al. Oxidase-deficient neutrophils from X-linked chronic granulomatous disease iPSC cells: functional correction by zinc finger nuclease-mediated safe harbor targeting. *Blood*. 2011;117(21):5561-72.
31. DeKaveler RC, Choi VM, Moehle EA, Paschon DE, Hockemeyer D, Meijsing SH, et al. Functional genomics, proteomics, and regulatory DNA analysis in isogenic settings using zinc finger nuclease-driven transgenesis into a safe harbor locus in the human genome. *Genome Res*. 2010;20(8):1133-42.
32. Hockemeyer D, Soldner F, Beard C, Gao Q, Mitalipova M, DeKaveler RC, et al. Efficient targeting of expressed and silent genes in human ESCs and iPSCs using zinc-finger nucleases. *Nat Biotechnol*. 2009;27(9):851-7.
33. Henckaerts E, Duthel N, Zeltner N, Kattman S, Kohlbrenner E, Ward P, et al. Site-specific integration of adeno-associated virus involves partial duplication of the target locus. *Proc Natl Acad Sci USA*. 2009;106(18):7571-6.
34. Ishikawa N, Okada S, Miki M, Shirao K, Kihara H, Tsumura M, et al. Neurodevelopmental abnormalities associated with severe congenital neutropenia due to the R86X mutation in the HAX1 gene. *J Med Genet*. 2008;45(12):802-7.

## Simple diagnosis of *STAT1* gain-of-function alleles in patients with chronic mucocutaneous candidiasis

Yoko Mizoguchi,<sup>\*,1</sup> Miyuki Tsumura,<sup>\*,1</sup> Satoshi Okada,<sup>\*,†</sup> Osamu Hirata,<sup>\*</sup> Shizuko Minegishi,<sup>‡</sup> Kohsuke Imai,<sup>§</sup> Nobuyuki Hyakuna,<sup>||</sup> Hideki Muramatsu,<sup>||</sup> Seiji Kojima,<sup>||</sup> Yusuke Ozaki,<sup>#</sup> Takehide Imai,<sup>#</sup> Sachiyo Takeda,<sup>#</sup> Tetsuya Okazaki,<sup>#</sup> Tsuyoshi Ito,<sup>\*\*</sup> Shin'ichiro Yasunaga,<sup>††</sup> Yoshihiro Takihara,<sup>††</sup> Vanessa L. Bryant,<sup>†</sup> Xiao-Fei Kong,<sup>†</sup> Sophie Cypowjy,<sup>†</sup> Stéphanie Boisson-Dupuis,<sup>†,‡‡</sup> Anne Puel,<sup>†‡</sup> Jean-Laurent Casanova,<sup>†,‡‡</sup> Tomohiro Morio,<sup>§</sup> and Masao Kobayashi<sup>\*,2</sup>

<sup>\*</sup>Department of Pediatrics, Hiroshima University Graduate School of Biomedical and Health Sciences, Japan; <sup>†</sup>St. Giles Laboratory of Human Genetics of Infectious Diseases, The Rockefeller University, New York, New York, USA; <sup>‡</sup>Division of Molecular Medicine, Institute for Genome Research, The University of Tokushima, Japan; <sup>§</sup>Department of Pediatrics and Developmental Biology, Graduate School of Medical and Dental Sciences, Tokyo Medical and Dental University, Japan; <sup>||</sup>Center of Bone Marrow Transplantation, Faculty of Medicine, University of the Ryukyus, Okinawa, Japan; <sup>¶</sup>Department of Pediatrics, Nagoya University Graduate School of Medicine, Japan; <sup>#</sup>Department of Pediatrics, Nippon Medical School, Tokyo, Japan; <sup>\*\*</sup>Department of Pediatrics, Toyohashi Municipal Hospital, Japan; <sup>††</sup>Department of Stem Cell Biology, Research Institute for Radiation Biology and Medicine, Hiroshima University, Japan; and <sup>‡‡</sup>Laboratory of Human Genetics of Infectious Diseases, Necker Branch, Necker Medical School, INSERM U980, and University Paris Descartes, Paris, France

RECEIVED MAY 5, 2013; REVISED NOVEMBER 13, 2013; ACCEPTED DECEMBER 2, 2013. DOI: 10.1189/jlb.0513250

### ABSTRACT

CMCD is a rare congenital disorder characterized by persistent or recurrent skin, nail, and mucosal membrane infections caused by *Candida albicans*. Heterozygous GOF *STAT1* mutations have been shown to confer AD CMCD as a result of impaired dephosphorylation of STAT1. We aimed to identify and characterize *STAT1* mutations in CMCD patients and to develop a simple diagnostic assay of CMCD. Genetic analysis of *STAT1* was performed in patients and their relatives. The mutations identified were characterized by immunoblot and reporter assay using transient gene expression experiments. Patients' leukocytes are investigated by flow cytometry and immunoblot. Six GOF mutations were identified, three of which are reported for the first time, that affect the CCD and DBD of *STAT1* in two sporadic and four multiplex cases in 10 CMCD patients from Japan. Two of the 10 patients presented with clinical symptoms atypical to CMCD, including other fungal and viral infections, and three patients developed bronchiectasis. Immunoblot analyses of pa-

tients' leukocytes showed abnormally high levels of pSTAT1 following IFN- $\gamma$  stimulation. Based on this finding, we performed a flow cytometry-based functional analysis of *STAT1* GOF alleles using IFN- $\gamma$  stimulation and the tyrosine kinase inhibitor, staurosporine. The higher levels of pSTAT1 observed in primary CD14<sup>+</sup> cells from patients compared with control cells persisted and were amplified by the presence of staurosporine. We developed a flow cytometry-based *STAT1* functional screening method that would greatly facilitate the diagnosis of CMCD patients with GOF *STAT1* mutations. *J. Leukoc. Biol.* **95**: 000–000; 2014.

### Introduction

Patients with CMCD suffer from persistent or recurrent skin, nail, and mucosal membrane infections caused by *C. albicans* [1, 2]. CMCD is also observed in patients with primary immunodeficiencies, such as T cell deficiencies, AD HIES, AR IL-12p40 deficiency, AR IL-12R $\beta$ 1 deficiency, and AR APS-1 [3–6]. Patients with AD HIES have very low levels of IL-17A- and IL-22-producing T cells as a result of an impairment of STAT3-mediated responses [7–10]. The numbers of IL-17A- and IL-22-producing T cells are also low in patients with IL-12p40 and IL-12R $\beta$ 1 deficiencies but to a lesser extent than in patients with AD HIES [8]. Patients with APS-1 develop high titers of

Abbreviations: AD=autosomal-dominant, APS-1=autoimmune polyendocrinopathy type 1 syndrome, AR=autosomal-recessive, CCD=coiled-coil domain, CMCD=chronic mucocutaneous candidiasis disease, DBD=DNA-binding domain, GAF= $\gamma$ -activating factor, GAS= $\gamma$ -activated sequence, GOF=gain-of-function, HIES=hyper-IgE syndrome, IRF=IFN regulatory factor, ISG=IFN-stimulated gene, ISRE=IFN-stimulated response element, MFI=mean fluorescence intensity, MSMD=mycobacterial disease, pSTAT1=phosphorylated STAT1, qPCR=quantitative PCR

The online version of this paper, found at [www.jleukbio.org](http://www.jleukbio.org), includes supplemental information.

1. These authors contributed equally to this manuscript.
2. Correspondence: Dept. of Pediatrics, Hiroshima University Graduate School of Biomedical Sciences, 1-2-3 Kasumi, Minami-ku, Hiroshima 734-8551, Japan. E-mail: masak@hiroshima-u.ac.jp

AQ: 4

neutralizing autoantibodies against IL-17A, IL-17F, and/or IL-22 [11, 12]. These findings suggest that human IL-17A, IL-17F, and/or IL-22 may be essential for mucocutaneous immunity to *C. albicans* [6]. This hypothesis led to the discovery of AR IL-17RA deficiency and AD IL-17F deficiency as genetic etiologies of CMCD without other severe infectious diseases (isolated CMCD) [13]. Thus, inborn errors of IL-17 immunity can underlie CMCD [14–17]. However, no genetic etiology has yet been identified for the vast majority of patients with CMCD.

Heterozygous mutations affecting the CCD of *STAT1* were identified recently by next-generation sequencing in patients with AD CMCD [18, 19]. A heterozygous T385M mutation, affecting the DBD of *STAT1*, was then discovered [20]. These mutations led to increases in Tyr701 p*STAT1*, GAF DNA-binding ability, and IFN- $\gamma$  transcription activity in response to IFN- $\gamma$ , IFN- $\alpha$ , and IL-27 [18, 20, 21]. Surprisingly, there, GOF *STAT1* alleles account for approximately one-half of patients with CMCD in previous studies (ref. [18] and unpublished results). The underlying molecular mechanism was deciphered using inhibitors of kinases and phosphatases and was shown to result from the impaired nuclear dephosphorylation of *STAT1* [18]. We report here six GOF *STAT1* mutations, three of which have never been described before, in two sporadic and four familial cases from four Japanese families with AD CMCD. We found that CD14<sup>+</sup> monocytes from the patients displayed persistent p*STAT1* in response to IFN- $\gamma$  and in the presence of the tyrosine kinase inhibitor staurosporine. Based on this observation, we developed a flow cytometry-based simple and rapid *STAT1* functional screening method to facilitate the diagnosis of CMCD patients with GOF *STAT1* mutations.

**MATERIALS AND METHODS**

**Patients**

Clinical information is summarized in Table 1. *STAT1* mutations identified in patients and familial segregation of *STAT1* mutations are shown in Fig. 1B.

**Kindred A (L354M/WT).** The proband (A-I-1: P1) is a 45-year-old man who has suffered from recurrent tinea unguium and otitis media since the age of 3 years. He also had several episodes of herpes virus infection, resulting in herpes simplex keratitis, dermatitis herpetiformis, and shingles during his childhood. At the age of 22, he experienced cryptococcal meningitis; he was diagnosed with hypothyroidism and placed on levothyroxine treatment. This patient also suffers from bronchiectasis and irritable bowel syndrome. His son is 7 years old (A-II-2) and suffers from recurrent oral aphthous lesions due to *C. albicans*. He has experienced no clinical episode suggestive of host susceptibility to viral or invasive fungal infection. At the age of 6 years, he was diagnosed with hypothyroidism and began treatment with levothyroxine. Both P1 and his son (A-II-2) have been found to have persistent, slightly high liver enzyme levels.

**Kindred B (M202V/WT).** The patient (B-II-1: P2) is a 34-year-old man with recurrent stomatitis as a result of *C. albicans* since infancy. He was diagnosed with CMCD at the age of 5 years. Oral itraconazole treatment was initiated at the age of 18 years, but this patient still suffers from persistent tinea unguium and oral candidiasis. He has suffered from bronchopneumonia more than twice yearly since his 20s. Sputum cultures were systematically negative for bacteria, but the bronchopneumonia seemed to respond to treatment with levofloxacin and cefotiam. No hypothyroidism has been detected.

**Kindred C (A267V/WT).** The proband (C-I-2: P3) is a 10-year-old boy. He developed onychomycosis at the age of 18 months and was treated with antifungal drugs for 6 months. He has presented no *Candida* infections since this episode. P3 had vascular purpura at the age of 6 years but does not have hypothyroidism. His mother (C-II-1) is 44 years old. She developed onychomycosis at the age of 1, vaginal candidiasis and tinea pedis at the age of 20, and recurrent oral candidiasis in her 30s, at which time, she

**TABLE 1. Summary of 10 Patients with CMCD from Six Kindred**

Patients	<i>STAT1</i> mutation	Fungal infections	Viral infection	Other complication
A-I-1	L354M	recurrent tinea unguium, cryptococcal meningitis	recurrent herpes virus infection	recurrent otiti media, bronchiectasis, irritable bowel syndrome, hypothyroidism, persistent, slightly elevated liver enzyme
A-II-2	L354M	recurrent oral aphthous as a result of <i>C. albicans</i>		hypothyroidism, persistent, slightly elevated liver enzyme
B-II-1	M202V	persistent tinea unguium, recurrent stomatitis as a result of <i>C. albicans</i>		bronchopneumonia
C-I-2	A267V	onychomycosis, tinea pedis, oral, esophageal, vaginal candidiasis		bronchiectasis, antiparietal cell antibody-positive megaloblastic anemia, hypothyroidism, persistent, slightly elevated liver enzyme
C-II-1	A267V	onychomycosis		vascular purpura
D-I-2	R274Q	recurrent oral and esophageal candidiasis, persistent skin candidiasis		
D-II-2	R274Q	oral candidiasis		
E-II-1	P329L	oral thrush		
E-II-2	P329L	recurrent oral thrush		pure red blood cell aplasia, autoimmune hemolytic anemia
F-II-1	M390T	recurrent oral and skin candidiasis	severe chicken-pox, chronic EBV infection	low serum IgG2 levels, bronchiectasis, mild hypothyroidism, recurrent severe diarrhea, recurrent otitis media, elevated liver enzyme

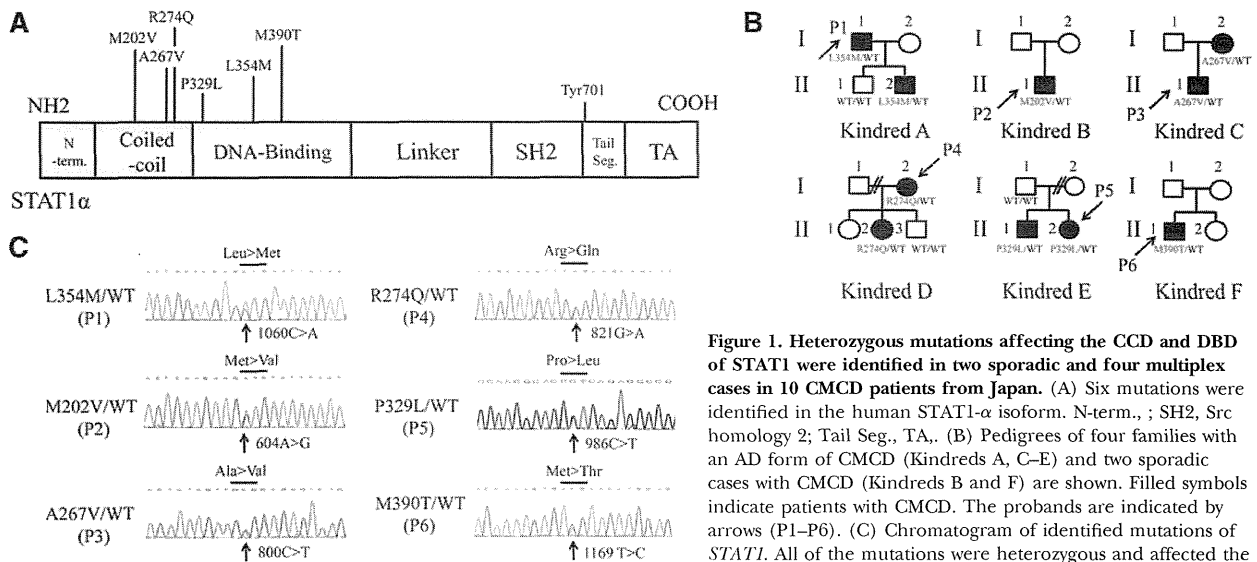


**Figure 1. Heterozygous mutations affecting the CCD and DBD of STAT1 were identified in two sporadic and four multiplex cases in 10 CMCD patients from Japan.** (A) Six mutations were identified in the human STAT1- $\alpha$  isoform. N-term., ; SH2, Src homology 2; Tail Seg., TA,. (B) Pedigrees of four families with an AD form of CMCD (Kindreds A, C–E) and two sporadic cases with CMCD (Kindreds B and F) are shown. Filled symbols indicate patients with CMCD. The probands are indicated by arrows (P1–P6). (C) Chromatogram of identified mutations of *STAT1*. All of the mutations were heterozygous and affected the CCD or DBD of STAT1.

was also diagnosed with bronchiectasis. At the age of 42 years, balloon dilatation was performed to relieve esophageal obstruction as a result of esophageal candidiasis. This patient also has hypothyroidism and antiparietal cell antibody-positive megaloblastic anemia. She was diagnosed with persistent slightly high liver enzyme levels.

**Kindred D (R274Q/WT).** The proband (D-I-2: P4) is a 32-year-old woman. She developed oral and cutaneous candidiasis at the age of 1 year and pneumonia with pleural effusion at the age of 10 years. The disease-causing pathogen was not identified, but the patient's symptoms improved rapidly after the initiation of antifungal treatments. Oral fluconazole treatment was introduced after this episode. However, the patient suffered from persistent skin candidiasis and recurrent esophageal candidiasis. Her second daughter (D-II-2) also suffers from oral candidiasis. This familial case was reported in a previous manuscript (Kindred H in ref. [18]).

**Kindred E (P329L/WT).** The proband (E-II-1: P5) is a 16-year-old girl who has suffered from recurrent oral thrush since infancy. At the age of 14 years, she displayed pure red blood cell aplasia and autoimmune hemolytic anemia, which responded to treatment with steroid and cyclosporine A. Her older brother (E-II-2) is 17 years old and has also suffered from oral thrush. Their father had no *STAT1* mutation, and no clinical or genetic information was available for their mother.

**Kindred F (M390T/WT).** The patient (F-II-1: P6) is a 30-year-old man with recurrent oral candidiasis since the age of 2 years. He suffered from severe chicken-pox at the age of 1 year, which took 90 days to resolve fully. He developed pneumonia at the age of 3 years, at which point, CMCD was suspected. After this episode, he suffered from recurrent, severe diarrhea, skin and oral candidiasis, and otitis media. The candidiasis was intractable despite treatment with antifungal drugs. At the age of 14 years, this patient was found to have low serum IgG2 levels and was given Ig replacement therapy. At the age of 17 years, he developed an impairment of liver function, and elevated liver enzyme was detected in serum. He also presented recurrent fever of unknown origin. He was found to have a high titer of EBV-transformed B cells in serum ( $1.9 \times 10^5$  copies/ml; reference range  $<1 \times 10^2$  copies/ml). He did not produce antibody against EBV nuclear antigen, which neutralizes EBV, during the clinical course of his illness, and chronic EBV infection was therefore suspected. This patient also has bronchiectasis and very mild hypothyroidism that does not require treatment. His parents and his younger sister do not present the clinical phenotype of CMCD.

### Molecular genetic analysis

Genomic DNA was extracted from peripheral blood leukocytes. Complete coding exons of *STAT1* and their flanking introns were amplified by PCR and sequenced. We inserted the various alleles of *STAT1* into the pCDNA3-V5 vector [18, 22, 23]. We also generated the P329L, L354M, and M390T mutations of *STAT1* by PCR-based mutagenesis with mismatched primers. Primer sequences and PCR conditions are available on request.

### Flow cytometric analysis

We assessed pSTAT1 in PBMCs from the patients. The MFI of pSTAT1 depended on the timing of the analysis. We therefore systematically assayed PBMCs, 24 h after blood collection. Mononuclear cells were suspended at a density of  $10^4$  cells/ $\mu$ l in serum-free RPMI. The cells were incubated with IFN- $\gamma$  (1000 U/ml) for 15 min. They were then washed and incubated with 0.5  $\mu$ M staurosporine (for 15 or 30 min for flow cytometry experiments and 15 min for immunoblot assays) in RPMI and subjected to analysis. For flow cytometry, the cells were stained simultaneously with anti-human CD3, CD19, or CD14 FITC antibody (BD PharMingen, San Diego, CA, USA) and treated with staurosporine. They were fixed and permeabilized, according to the BD Phosflow protocol (Protocol III); stained with FITC-conjugated anti-CD3, CD19, or CD14 and PE-conjugated anti-pSTAT1 (BD PharMingen) antibodies; and subjected to flow cytometric analysis. It took 6 h to perform the complete flow cytometric analysis.

### Immunoblot analysis and EMSA

STAT1-null U3C fibrosarcoma cells were maintained in DMEM, supplemented with 10% FBS. The cells were harvested and replated at a density of  $2.5 \times 10^5$  cells/ml in six-well culture plates. After incubation for a further 24 h, plasmid DNA (5  $\mu$ g/well), carrying the WT or a mutant STAT1 allele, was introduced into the cells by calcium phosphate-mediated transfection. The transfected cells were incubated for 24 h, and  $10^4$  IU/ml IFN- $\gamma$  was then added. The cells were incubated for a further 15 min and then subjected for EMSA and immunoblot analysis. Immunoblot analysis was performed as described previously [24]. The primary antibodies used were an anti-pSTAT1 (pY701) antibody (BD Biosciences, San Jose, CA, USA; Cell Signaling Technology, Danvers, MA, USA); an anti-STAT1 antibody (C-24; Santa Cruz Biotechnology, Santa Cruz, CA, USA); and an anti-

$\beta$ -actin antibody (Sigma-Aldrich, St. Louis, MO, USA). EMSA was carried out as described previously [24]. After IFN- $\gamma$  stimulation, U3C-transfected cells were subjected to nuclear extraction. We incubated 20  $\mu$ g nuclear extract with  $^{32}$ P-labeled ( $\alpha$ -dATP) GAS (produced under control for the *FCGR1* promoter) probe for 30 min.

### Luciferase reporter assay

Luciferase assays were performed as described previously [18, 22, 23]. Briefly, transfected U3C cells were stimulated with IFN- $\alpha$  (5000 IU/ml), IL-27 (20 mg/ml), or various concentrations of IFN- $\gamma$  (1, 5, 10, 50, 100, 500, and 1000 IU/ml) for 8 h and then analyzed. The data are expressed as fold inductions with respect to unstimulated cells. Experiments were performed in triplicate.

### qPCR analysis

CD14<sup>+</sup> monocytes were purified from PBMCs by magnetic sorting (BD Biosciences) and stimulated with 1000 IU/ml IFN- $\gamma$  for 2 or 8 h. Then, total RNA was extracted and used for reverse transcription with random primers to generate cDNA. IRF1, CXCL9, and ISG15 mRNA levels were determined by qPCR with Taqman probes. The results were normalized with respect to the values obtained for the endogenous GAPDH cDNA.

### Statistical analysis

Statistical significance was analyzed by nonparametric Mann-Whitney U-tests and variance followed by Tukey's post hoc analysis using SPSS software. For all analyses,  $P < 0.05$  was considered statistically significant.

## RESULTS

### Identification of *STAT1* mutations

We investigated five sporadic and five familial cases of CMCD from a total of 15 patients from 10 kindreds. Heterozygous *STAT1* mutations were identified in two sporadic and four familial cases (and four additional cases were identified among affected relatives who were subsequently recruited, giving a total of 10 patients). Thus, *STAT1* mutations were commonly identified in Japanese patients with CMCD. We identified three previously unknown heterozygous mutations of *STAT1*: c.1060C > A (L354M) in P1 and his younger son (A-II-2), c.986C > T (P329L) in P5 and her elder brother (E-II-2), and c.1169T > C (M390T) in P6 (Fig. 1C). We also identified previously reported heterozygous mutations: c.604A > G (M202V) in P2 and c.800C > T (A267V) in P3 and her son (C-II-1) [18, 19]. The c.821G > A (R274Q) mutation was identified in P4 and her second daughter (D-II-2). This familial case is reported in a previous manuscript (Kindred K in ref. [18]). None of these mutations were identified in the healthy relatives tested, suggesting that clinical penetrance was complete. The newly identified mutations, P329L, L354M, and M390T, were not found in the National Center for Biotechnology Information, Ensembl, or dbSNP databases. They were also absent from 1052 controls from 52 ethnic groups in the Centre d'Étude du Polymorphisme Humain and Human Genome Diversity panels. These three mutations are thus rare variants rather than common, irrelevant polymorphisms segregating with AD CMCD.

### Impairment of *STAT1* Tyr701 dephosphorylation in PBMCs

Previous in vitro studies suggested that CMCD-related *STAT1* mutations impair nuclear dephosphorylation [18]. However,

only few reports investigate dephosphorylation of *STAT1* in primary cells from the patients ex vivo [25, 26]. We analyzed p*STAT1* protein in PBMCs from P4, P5, and two healthy controls. As shown in Fig. 2A, *STAT1* protein levels were normal in the CMCD patients' PBMCs. The patients' cells contained some p*STAT1* in the absence of stimulation, and the levels of p*STAT1* increased strongly in response to IFN- $\gamma$  stimulation, remaining high after treatment with the tyrosine kinase inhibitor staurosporine, which inhibits JAK-*STAT* signaling upstream of *STAT1*, probably as a result of impaired nuclear *STAT1* dephosphorylation. The upper and lower bands correspond to *STAT1* $\alpha$  and *STAT1* $\beta$  in the p*STAT1* blot, whereas the bands correspond to *STAT1* $\alpha$  in the *STAT1* blot.

We first investigated IFN- $\gamma$ -induced p*STAT1* by flow cytometry, using various subsets isolated from PBMCs from healthy controls and patients with CMCD (Supplemental Fig. 1). A high level of p*STAT1* was observed in CD14<sup>+</sup> monocytes, whereas it was not obvious in CD3<sup>+</sup> T cells or CD19<sup>+</sup> B cells. These observations were highly consistent with the data of previous studies [27–30]. Patients' cells showed a higher level of IFN- $\gamma$ -induced p*STAT1* compared with healthy control. We therefore investigated *STAT1* dephosphorylation focusing on CD14<sup>+</sup> monocytes. As the *STAT1* GOF mutations are thought to be associated with impairment in dephosphorylation of *STAT1* [16], we used staurosporine to clarify the difference between *STAT1* WT alleles and *STAT1* GOF alleles. If the *STAT1* dephosphorylation normally occurs in the nucleus, then p*STAT1* should decrease promptly following staurosporine treatment. Most of the patient blood samples were available only 24 h of transport. To control for the effect of time of blood processing on p*STAT1* and *STAT1* dephosphorylation, we studied PBMCs from the same donor under two conditions: immediately after collection of blood samples or after a delay of 24 h (Supplemental Fig. 2). The level of p*STAT1* decreased in all of the conditions tested in the blood samples that were delayed. Thus, we decided to perform all assays in PBMCs, isolated and tested 24 h after blood collection. PBMCs from one patient with CMCD, carrying a WT *STAT1* allele; 14 healthy individuals; and 10 GOF *STAT1* patients—five from Kindreds A–C and five CMCD patients from another cohort carrying GOF *STAT1* mutations (nonreported cases)—were incubated with IFN- $\gamma$  for 15 min. The cells were then washed and incubated with staurosporine-containing media for 15 min prior to analysis. For P1 only, we also measured p*STAT1* after 30 min of staurosporine treatment. Figure 2B shows a representative histogram comparing P1 and control. CD14<sup>+</sup> monocytes from P1 had higher levels of p*STAT1* than control cells following IFN- $\gamma$  stimulation. The CD14<sup>+</sup> monocytes from the control displayed rapid *STAT1* dephosphorylation, whereas p*STAT1* persisted in the patients' monocytes in the presence of staurosporine. Residual p*STAT1* was found in the cells of P1, even after 30 min of treatment with staurosporine. The summary of MFI values for p*STAT1* obtained by flow cytometry is shown in Fig. 2C. Some overlap was observed, but levels of p*STAT1*, in response to IFN- $\gamma$ , were significantly higher in CD14<sup>+</sup> cells from the patients than in those from the controls ( $*P < 0.001$ ). In the absence of stimulation, p*STAT1* levels were higher in the patients' cells than in control cells ( $*P < 0.011$ ).

AQ: 2

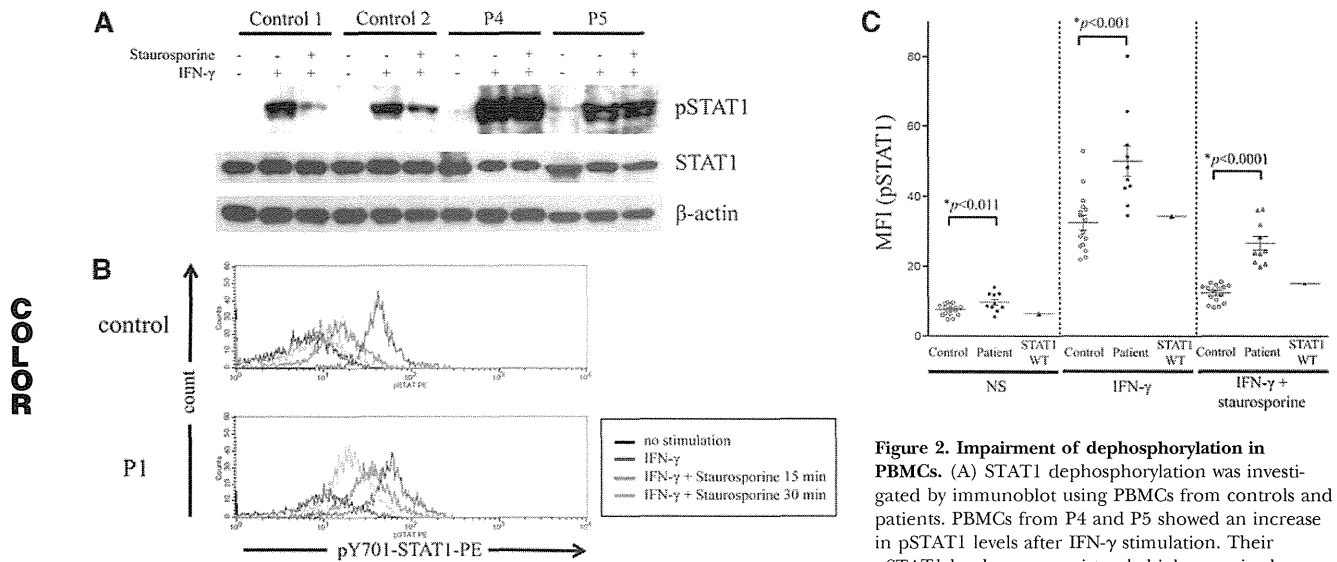


**Figure 2. Impairment of dephosphorylation in PBMCs.** (A) STAT1 dephosphorylation was investigated by immunoblot using PBMCs from controls and patients. PBMCs from P4 and P5 showed an increase in pSTAT1 levels after IFN- $\gamma$  stimulation. Their pSTAT1 levels were persistently high, even in the pres-

ence of staurosporine. Immunoblot analysis was carried out twice to confirm the results. (B and C) PBMCs from the 10 patients, 14 healthy individuals, and one patient with CMCD, carrying a WT *STAT1* allele, were stimulated with IFN- $\gamma$  and incubated in the presence of staurosporine. The cells were stained with anti-CD14 and anti-pY701 STAT1 antibodies and analyzed by flow cytometry with gating on CD14. The figures show a representative histogram of pSTAT1 intensity (B) and a summary of the MFI of pSTAT1 (C). (B) Black line, No stimulation; blue line, IFN- $\gamma$  for 15 min; red and orange lines, incubation with staurosporine for 15 or 30 min, respectively, after IFN- $\gamma$  stimulation.

This excess phosphorylation persisted after 15 min of treatment with staurosporine, a tyrosine kinase inhibitor ( $*P < 0.0001$ ). Moreover, in these conditions, there was no overlap in MFI of pSTAT1 between the patients and healthy controls or with a CMCD patient carrying a WT *STAT1* allele. The atypical clinical signs observed in the patients did not affect the results of flow cytometric analysis. The difference in the percentage decrease in pSTAT1 levels in the presence of staurosporine between healthy controls and patients was significant too ( $*P < 0.02$ ; Supplemental Fig. 3). These results clearly indicate that the dephosphorylation process is impaired in CMCD patients. The flow cytometric analysis of pSTAT1 levels in monocytes has been established previously as a screening tool to identify IFN- $\gamma$  signaling defects in patients with Mendelian susceptibility to MSMDs [31]. Taken together, this flow cytometry-based technique is likely to be useful for the rapid assessment of *STAT1* function in CMCD patients.

### Induction of ISGs in CD14<sup>+</sup> monocytes

We investigated the induction of ISGs in patients' cells by purifying CD14<sup>+</sup> monocytes, stimulating them with IFN- $\gamma$ , and assessing the expression of the downstream ISGs *CXCL9*, *IRF1*, and *ISG15* by RT-qPCR analysis (Fig. 3). The induction of these three ISGs has been shown to be *STAT1*-dependent in previous studies [22–24, 32, 33]. CD14<sup>+</sup> monocytes from patients with CMCD (P2 and P4 and a patient carrying a R274W mutation from another cohort) showed a significantly higher induction of *CXCL9* and *IRF1* expression than did those of healthy controls. By contrast, we did not see a significant increase in the induction of *ISG15* in the patients. These results suggest that the mutated *STAT1* alleles identified in CMCD

patients are GOF in terms of the induction of transcription for many, but probably not all, downstream ISGs.

### Increased pSTAT1 and GAF DNA-binding ability

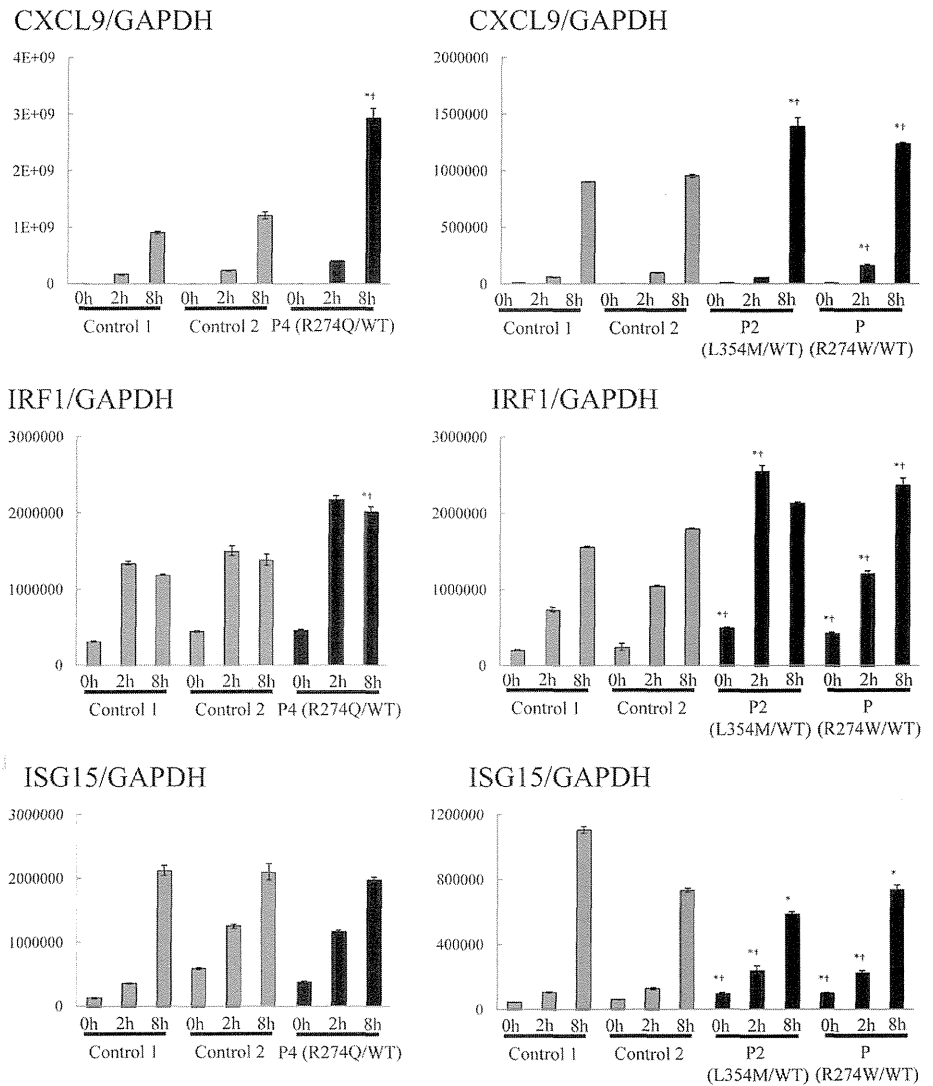
For confirmation of the *STAT1* gain-of-phosphorylation observed in primary cells from the patients, we investigated *STAT1*-dependent signaling pathways by transiently transfecting *STAT1*-null U3C fibrosarcoma cells. *STAT1* protein production was normal for the CMCD-related *STAT1* mutants (Fig. 4A). Upon IFN- $\gamma$  stimulation, all of the mutant proteins displayed higher levels of pSTAT1, at least a 1.5-fold increase over WT, as determined by densitometry (Supplemental Fig. 4). As expected, phosphorylation of the MSMD-related mutant, L706S *STAT1*, was impaired [34]. Thus, all of the CMCD-related mutations identified resulted in a gain of phosphorylation in response to IFN- $\gamma$ . Next, we assessed the DNA-binding ability of the mutant *STAT1* proteins to the GAS sequence using the same transfected cells, which were subjected to immunoblot analysis (Fig. 4B). All mutants, including the three mutations identified in the DBD, displayed GOF properties, resulting in an increase of GAF binding to DNA. However, the DNA binding to GAS was abolished in the MSMD-related mutant, L706S *STAT1*.

### Transcriptional activity of the CMCD-related *STAT1* mutant protein

Transcriptional activity was studied by transfecting U3C cells with reporter plasmids and plasmids carrying the WT and/or



**Figure 3. The induction of ISGs in CD14<sup>+</sup> monocytes.** CD14<sup>+</sup> monocytes from P4 and two healthy controls were stimulated with 1000 U/ml IFN- $\gamma$  (2 or 8 h), and the expression of the downstream ISGs *CXCL9*, *IRF1*, and *ISG15* was assessed by RT-qPCR. Much stronger induction of *CXCL9* and *IRF1* was observed in the patients' cells than in control cells, whereas there was no significant increase in *ISG15* induction. The expression of ISGs was normalized with respect to that of endogenous *GAPDH*. The results are representative of three independent experiments, except for the CD14<sup>+</sup> monocyte experiment (performed twice). Differences were statistically significant in the cells expressing the mutant *STAT1*s compared with Control 1 cells (\* $P < 0.05$ ) and Control 2 cells ( $\dagger P < 0.05$ ).

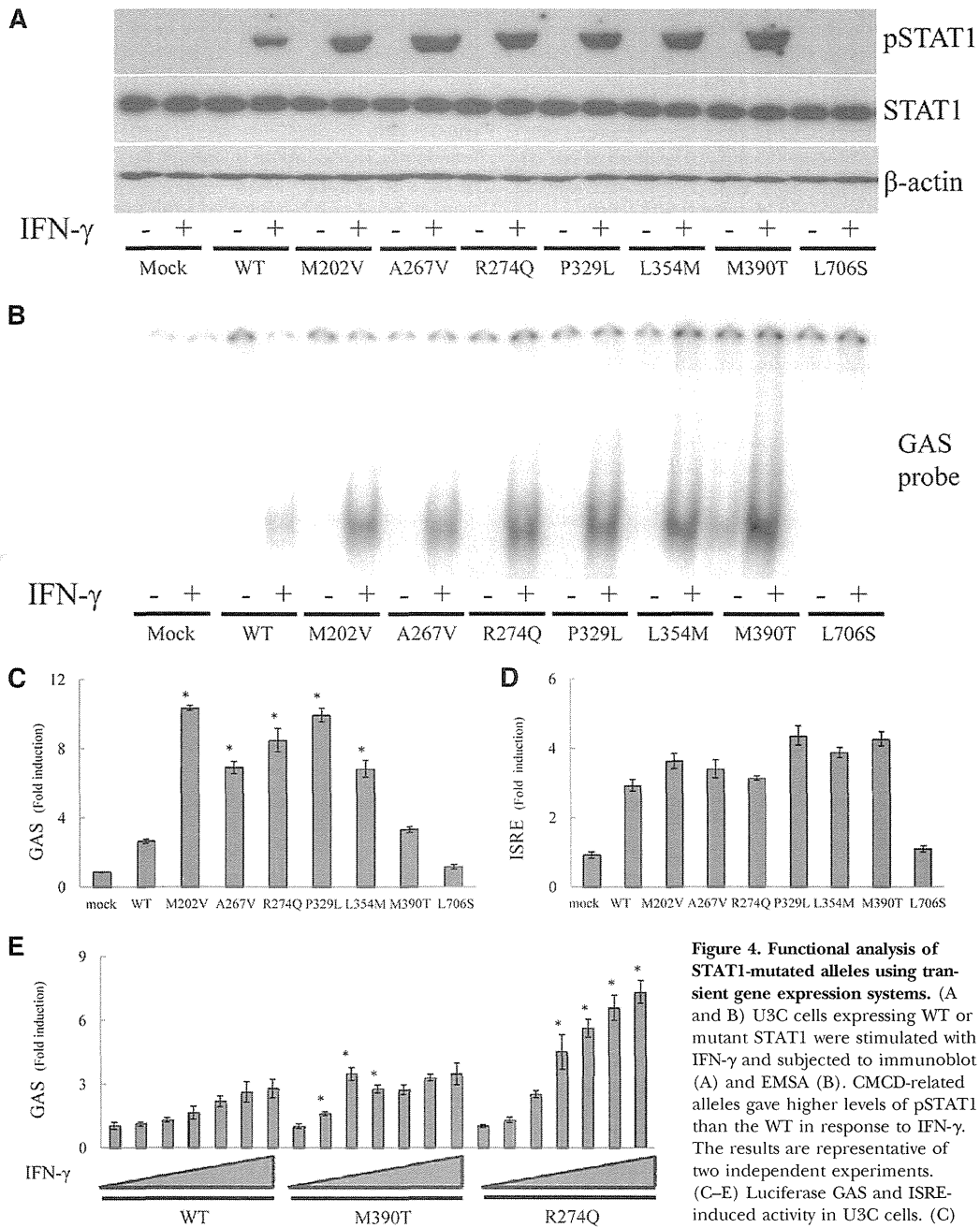


mutant alleles of *STAT1*. The cells transfected with the CMCD-related alleles, except for M390T, had levels of GAS transcriptional activity in response to IFN- $\gamma$ , more than twice those of cells transfected with the WT allele (Fig. 4C). The L706S MSMD-related *STAT1* allele abolished the transcriptional activity of GAS. The increase in GAS transcriptional activity was only slight for the M390T protein in this condition. However, the GOF became obvious when the cells were stimulated with low concentrations of IFN- $\gamma$  (Fig. 4E). We also investigated IL-27-induced GAS activation (Supplemental Fig. 5) and confirmed excess GAS induction in all of the CMCD-related mutations. We then assessed ISRE transcription activity in response to IFN- $\alpha$  (Fig. 4D). Some positive effects on ISRE transcription activity were suspected in CMCD-related mutations, but they were not statistically significant. Thus, all of the CMCD-related mutations caused a GOF-to-GAS-mediated transcription. More-

over, the GOF was more marked at lower concentrations of IFN- $\gamma$ .

## DISCUSSION

In this study, *STAT1* mutations were identified with a high frequency (almost 70%) in Japanese CMCD patients; we identified heterozygous *STAT1* mutations in two of five sporadic cases and in eight of 10 cases from five multiplex kindreds. In total, we identified 10 CMCD patients with GOF *STAT1* mutations from a total of 15 diseased individuals. *STAT1* mutations were also found in ~50% of the patients with CMCD, identified in a previous study investigating large numbers of patients from numerous countries (ref. [18] and unpublished results). It remains possible that the frequency of *STAT1* mutations is



GRAYSCALE

**Figure 4. Functional analysis of STAT1-mutated alleles using transient gene expression systems.** (A and B) U3C cells expressing WT or mutant STAT1 were stimulated with IFN- $\gamma$  and subjected to immunoblot (A) and EMSA (B). CMCD-related alleles gave higher levels of pSTAT1 than the WT in response to IFN- $\gamma$ . The results are representative of two independent experiments. (C-E) Luciferase GAS and ISRE-induced activity in U3C cells. (C) All of the CMCD-related STAT1

mutations, except for M390T, were associated with levels of GAS transcriptional activity in response to IFN- $\gamma$ , at least twice as high as those in cells transfected with the WT allele. (E) The M390T STAT1 behaved as a GOF protein in response to stimulation with low concentrations of IFN- $\gamma$ . (D) An increase in ISRE induction in response to IFN- $\alpha$  was also observed in CMCD-related mutants, but this increase was much smaller than that observed for GAS induction. Differences were statistically significant in the cells expressing the mutants compared with the WT-expressing cells (\* $P$ <0.05).

overestimated here as a result of the limited number of cases in our cohort, but these results nevertheless strongly suggest that STAT1 GOF is the most frequent genetic etiology of CMCD among Japanese patients, accounting for at least one-half of these patients. The clinical penetrance of *STAT1* mutations appears to be extremely high, if not complete, as no individual with the morbid genotype but not CMCD has ever been identified [18–21, 35, 36]. We observed differences in clinical signs and severity, even between siblings with the same *STAT1* mutation. All of the mutated alleles, including three previously unknown mutations, were gain-of-phosphorylation and GOF in vitro in terms of GAS transcriptional activity. Moreover, all of these mutations affected residues in the CCD or DBD of STAT1. These results are highly consistent with previous findings [18–21, 35, 36].

Levels of pSTAT1 were found to be persistently high in the patients' CD14<sup>+</sup> monocytes by flow cytometric analysis. STAT1 does not appear to be hyperphosphorylated in lymphocytes but rather, in myeloid cells from patients with CMCD. A high level of pSTAT1 can be explained by the strong IFN- $\gamma$ R2 surface expression, specifically on monocytes, whereas IFN- $\gamma$ R1 is expressed ubiquitously [30]. The patients' cells had high basal levels of pSTAT1, a finding confirmed by immunoblot analysis of the patients' PBMCs. The amount of pSTAT1 in the cell is determined by the balance between pSTAT1 and STAT1 dephosphorylation [37]. CMCD-related mutations impair STAT1 nuclear dephosphorylation, potentially leading to some accumulation of pSTAT1 even in the absence of stimulation. Following stimulation with IFN- $\gamma$ , CD14<sup>+</sup> monocytes contained significantly larger amounts of pSTAT1 than control cells. Moreover, this difference in pSTAT1 levels was even greater when staurosporine was added after IFN- $\gamma$  stimulation. Higher levels of IFN- $\gamma$ -induced pSTAT1 in monocytes of CMCD patients overlap with levels detected in cells from normal subjects, and the addition of staurosporine is required to discriminate the CMCD patients from control subjects. This technique is likely to be useful for the rapid assessment of STAT1 function in CMCD patients with unknown genetic etiology or those carrying functionally uncharacterized *STAT1* mutations. Furthermore, the results obtained are not affected by clinical diversity in the patients. Given the high frequency of GOF mutations of *STAT1*, the establishment of a rapid screening system based on STAT1 function should greatly facilitate the diagnosis of patients with CMCD.

Two patients presented atypical clinical signs in addition to CMCD. P1 suffered from cryptococcal meningitis, shingles, herpes simplex keratitis, and dermatitis. P6 presented severe, prolonged chicken-pox and chronic EBV infection. *Cryptococcus* is an opportunistic fungal pathogen, and IFN- $\gamma$  signaling may play an important role in protective immunity against this microbe [38]. Indeed, IFN- $\gamma$  administration increases the rate of clearance of HIV-associated cryptococcal infection from the cerebrospinal fluid when combined with antifungal drugs [39]. The CMCD-related *STAT1* mutations observed here were GOF in terms of IFN- $\gamma$ -induced GAS transcriptional activity in vitro, so the cryptococcal meningitis observed in this patient is paradoxical. In addition to our study, recurrent cutaneous fusariosis and disseminated coccidioidomycosis and histoplas-

mosis have been reported in patients with GOF *STAT1* mutation [40, 41]. Viral infections have also been reported in CMCD patients: one case of symptomatic cytomegalovirus infection and one familial case with recurrent herpes simplex virus and varicella infections have been reported [19, 25, 36]. STAT1 mediates the IFN- $\alpha/\beta$ -induced transcription of ISRE, which plays an important role in antiviral immunity. Therefore, severe viral infection is one of the typical symptoms in patients with AR *STAT1* deficiency, which is caused by loss-of-function or hypomorphic mutations of *STAT1* [23, 32, 42–44]. As the CMCD-related *STAT1* mutations presented normal activity in terms of IFN- $\alpha$ -induced ISRE transcriptional activity in vitro, viral infections observed in two patients are also paradoxical. We observed higher levels of induction for *CXCL9* and *IRF1*, but not *ISG15*, in response to IFN- $\gamma$  in CD14<sup>+</sup> monocytes from CMCD patients than in those from controls. These results suggest that *STAT1* GOF mutations may not induce an increase in the transcription of all downstream ISGs, potentially even causing paradoxical patterns of regulation for some target genes. There may be similar paradoxical responses to IFN- $\alpha/\beta$ , at least for some target genes. Moreover, a recent report suggests that the induction of *CXCL9* and *CXCL10* is impaired in *STAT1*-deficient U3A cells expressing GOF *STAT1* alleles upon specific conditions, such as the restimulation with IFN- $\gamma$  [41]. Further studies are required to determine whether and how *STAT1* GOF mutations confer a predisposition to pathogens, for which clearance generally requires normal IFN- $\gamma$  and/or IFN- $\alpha$  signaling.

Surprisingly, a very recent report identified GOF mutations in *STAT1* in patients with *forkhead box P3* WT immune dysregulation, polyendocrinopathy, autoimmune enteropathy, and X-linked-like syndrome [25]. These patients present a broad, infectious phenotype that may be explained partially by progressive lymphopenia, finally resulting in hypogammaglobulinemia [26]. Although progressive lymphopenia was not observed, the patients in our cohort also presented a broad, infectious phenotype. Taken together with the clinical cases presented in our current study, these findings suggest that GOF mutations of *STAT1* may be associated with a much broader infectious phenotype than thought initially.

## AUTHORSHIP

Y.M., M.T., S.O., O.H., and S.M. were involved in research design and data analysis. Y.M. and S.O. wrote the manuscript. K.I., N.H., H.M., S.K., Y.O., T. Imai, S.T., T.O., and T. Ito treated the patients. S.Y., Y.T., V.L.B., X-F.K., S.C., S.B-D., A.P., J-L.C., T.M., and M.K. directed experiments and edited the paper. S.O., T.M., and M.K. supervised all work.

## ACKNOWLEDGMENTS

This study was supported, in part, by Grants-in-Aid for Scientific Research from the Japan Society for the Promotion of Science (22591161 to M.K.) and by Research on Measures for Intractable Diseases funding from the Japanese Ministry of

Health, Labor and Welfare (H22-Nanchi-ippan-078 to M.K.). This study was also supported, in part, by The Rockefeller University and grants from the National Center for Research Resources; National Center for Advancing Sciences (NCATS), U.S. National Institutes of Health (Grant Number 8UL1TR000043); and St. Giles Foundation. S.C. was supported by the AXA Research Fund and V.L.B and X-F.K., by the Stony Wold-Herbert Fund. Sequence analysis was supported by the Analysis Center of Life Science, Natural Science Center for Basic Research and Development, Hiroshima University. We thank Dr. Yoshiko Hasii (Osaka University) for referring patients. We thank Dusan Bogunovic, Alexandra Kreins, Marcela Moncada Velez, Ruben Martinez-Barriarte, and Michael Ciancanelli for helpful discussions and critical reading. We thank the members of the laboratory, Yelena Nemirovskaya and Eric Anderson, for secretarial assistance and Tiffany Nivare for technical assistance.

#### DISCLOSURES

The authors declare no conflict of interest.

#### REFERENCES

- Kirkpatrick, C. H. (2001) Chronic mucocutaneous candidiasis. *Pediatr. Infect. Dis. J.* **20**, 197–206.
- Lilic, D. (2002) New perspectives on the immunology of chronic mucocutaneous candidiasis. *Curr. Opin. Infect. Dis.* **15**, 143–147.
- Minegishi, Y., Saito, M., Tsuchiya, S., Tsuge, I., Takada, H., Hara, T., Kawamura, N., Ariga, T., Pasic, S., Stojkovic, O., Metin, A., Karasuyama, H. (2007) Dominant-negative mutations in the DNA-binding domain of STAT3 cause hyper-IgE syndrome. *Nature* **448**, 1058–1062.
- Holland, S. M., DeLeo, F. R., Elloumi, H. Z., Hsu, A. P., Uzel, G., Brodsky, N., Freeman, A. F., Demidowich, A., Davis, J., Turner, M. L., et al. (2007) STAT3 mutations in the hyper-IgE syndrome. *N. Engl. J. Med.* **357**, 1608–1619.
- De Beaucoudrey, L., Samarina, A., Bustamante, J., Cobat, A., Boisson-Dupuis, S., Feinberg, J., Al-Muhsen, S., Jannié, L., Rose, Y., de Suremain, M., et al. (2010) Revisiting human IL-12RB1 deficiency: a survey of 141 patients from 30 countries. *Medicine (Baltimore)* **89**, 381–402.
- Puel, A., Picard, C., Cypowij, S., Lilic, D., Abel, L., Casanova, J. L. (2010) Inborn errors of mucocutaneous immunity to *Candida albicans* in humans: a role for IL-17 cytokines? *Curr. Opin. Immunol.* **22**, 467–474.
- Minegishi, Y., Saito, M., Nagasawa, M., Takada, H., Hara, T., Tsuchiya, S., Agematsu, K., Yamada, M., Kawamura, N., Ariga, T., Tsuge, I., Karasuyama, H. (2009) Molecular explanation for the contradiction between systemic Th17 defect and localized bacterial infection in hyper-IgE syndrome. *J. Exp. Med.* **206**, 1291–1301.
- De Beaucoudrey, L., Puel, A., Filipe-Santos, O., Cobat, A., Ghandil, P., Chrabieh, M., Feinberg, J., von Bernuth, H., Samarina, A., Jannié, L., et al. (2008) Mutations in STAT3 and IL12RB1 impair the development of human IL-17-producing T cells. *J. Exp. Med.* **205**, 1543–1550.
- Milner, J. D., Brenchley, J. M., Laurence, A., Freeman, A. F., Hill, B. J., Elias, K. M., Kanno, Y., Spalding, C., Elloumi, H. Z., Paulson, M. L., Davis, J., Hsu, A., Asher, A. L., O'Shea, J., Holland, S. M., Paul, W. E., Douek, D. C. (2008) Impaired T(H)17 cell differentiation in subjects with autosomal dominant hyper-IgE syndrome. *Nature* **452**, 773–776.
- Ma, C. S., Chew, G. Y., Simpson, N., Priyadarshi, A., Wong, M., Grimbacher, B., Fulcher, D. A., Tangye, S. G., Cook, M. C. (2008) Deficiency of Th17 cells in hyper IgE syndrome due to mutations in STAT3. *J. Exp. Med.* **205**, 1551–1557.
- Kisand, K., Boe Wolff, A. S., Podkrajsek, K. T., Tserel, L., Link, M., Kisand, K. V., Ersvaer, E., Perheentupa, J., Erichsen, M. M., Bratanic, N., et al. (2010) Chronic mucocutaneous candidiasis in APECED or thymoma patients correlates with autoimmunity to Th17-associated cytokines. *J. Exp. Med.* **207**, 299–308.
- Puel, A., Doffinger, R., Natividad, A., Chrabieh, M., Barcenas-Morales, G., Picard, C., Cobat, A., Ouachee-Charadin, M., Toulon, A., Bustamante, J., et al. (2010) Autoantibodies against IL-17A, IL-17F, and IL-22 in patients with chronic mucocutaneous candidiasis and autoimmune polyendocrine syndrome type I. *J. Exp. Med.* **207**, 291–297.
- Puel, A., Cypowij, S., Bustamante, J., Wright, J. F., Liu, L., Lim, H. K., Migaud, M., Israel, L., Chrabieh, M., Audry, M., et al. (2011) Chronic mucocutaneous candidiasis in humans with inborn errors of interleukin-17 immunity. *Science* **332**, 65–68.
- Cypowij, S., Picard, C., Marodi, L., Casanova, J. L., Puel, A. (2012) Immunity to infection in IL-17-deficient mice and humans. *Eur. J. Immunol.* **42**, 2246–2254.
- Marodi, L., Cypowij, S., Toth, B., Chernyshova, L., Puel, A., Casanova, J. L. (2012) Molecular mechanisms of mucocutaneous immunity against *Candida* and *Staphylococcus* species. *J. Allergy Clin. Immunol.* **130**, 1019–1027.
- Puel, A., Cypowij, S., Marodi, L., Abel, L., Picard, C., Casanova, J. L. (2012) Inborn errors of human IL-17 immunity underlie chronic mucocutaneous candidiasis. *Curr. Opin. Allergy Clin. Immunol.* **12**, 616–622.
- Alcais, A., Quintana-Murci, L., Thaler, D. S., Schurr, E., Abel, L., Casanova, J. L. (2010) Life-threatening infectious diseases of childhood: single-gene inborn errors of immunity? *Ann. N. Y. Acad. Sci.* **1214**, 18–33.
- Liu, L., Okada, S., Kong, X. F., Kreins, A. Y., Cypowij, S., Abhyankar, A., Toubiana, J., Itan, Y., Audry, M., Nitschke, P., et al. (2011) Gain-of-function human STAT1 mutations impair IL-17 immunity and underlie chronic mucocutaneous candidiasis. *J. Exp. Med.* **208**, 1635–1648.
- Van de Veerdonk, F. L., Plantinga, T. S., Hoischen, A., Smeekens, S. P., Joosten, L. A., Gilissen, C., Arts, P., Rosentul, D. C., Carmichael, A. J., Smits-van der Graaf, C. A., Kullberg, B. J., van der Meer, J. W., Lilic, D., Veltman, J. A., Netea, M. G. (2011) STAT1 mutations in autosomal dominant chronic mucocutaneous candidiasis. *N. Engl. J. Med.* **365**, 54–61.
- Takezaki, S., Yamada, M., Kato, M., Park, M. J., Maruyama, K., Yamazaki, Y., Chida, N., Ohara, O., Kobayashi, I., Ariga, T. (2012) Chronic mucocutaneous candidiasis caused by a gain-of-function mutation in the STAT1 DNA-binding domain. *J. Immunol.* **189**, 1521–1526.
- Smeekens, S. P., Plantinga, T. S., van de Veerdonk, F. L., Heinhuis, B., Hoischen, A., Joosten, L. A., Arkwright, P. D., Gennery, A., Kullberg, B. J., Veltman, J. A., Lilic, D., van der Meer, J. W., Netea, M. G. (2011) STAT1 hyperphosphorylation and defective IL12R/IL23R signaling underlie defective immunity in autosomal dominant chronic mucocutaneous candidiasis. *PLoS One* **6**, e29248.
- Chappier, A., Boisson-Dupuis, S., Jouanguy, E., Vogt, G., Feinberg, J., Prochnicka-Chaloufour, A., Casrouge, A., Yang, K., Soudais, C., Fieschi, C., et al. (2006) Novel STAT1 alleles in otherwise healthy patients with mycobacterial disease. *PLoS Genet.* **2**, e131.
- Kong, X. F., Ciancanelli, M., Al-Hajjar, S., Alsina, L., Zumwalt, T., Bustamante, J., Feinberg, J., Audry, M., Prando, C., Bryant, V., et al. (2010) A novel form of human STAT1 deficiency impairing early but not late responses to interferons. *Blood* **116**, 5895–5906.
- Tsumura, M., Okada, S., Sakai, H., Yasunaga, S., Ohtsubo, M., Murata, T., Obata, H., Yasumi, T., Kong, X. F., Abhyankar, A., et al. (2012) Dominant-negative STAT1 SH2 domain mutations in unrelated patients with Mendelian susceptibility to mycobacterial disease. *Hum. Mutat.* **33**, 1377–1387.
- Uzel, G., Sampaio, E. P., Lawrence, M. G., Hsu, A. P., Hackett, M., Dorsey, M. J., Noel, R. J., Verbsky, J. W., Freeman, A. F., Jansen, E., et al. (2013) Dominant gain-of-function STAT1 mutations in FOXP3 wild-type immune dysregulation-polyendocrinopathy-enteropathy-X-linked-like syndrome. *J. Allergy Clin. Immunol.* **131**, 1611–1623.
- Rombert, N., Morbach, H., Lawrence, M. G., Kim, S., Kang, I., Holland, S. M., Milner, J. D., Meffre, E. (2013) Gain-of-function STAT1 mutations are associated with PD-L1 overexpression and a defect in B-cell survival. *J. Allergy Clin. Immunol.* **131**, 1691–1693.
- Bernabei, P., Coccia, E. M., Rigamonti, L., Bosticardo, M., Forni, G., Pestka, S., Krause, C. D., Battistini, A., Novelli, F. (2001) Interferon- $\gamma$  receptor 2 expression as the deciding factor in human T, B, and myeloid cell proliferation or death. *J. Leukoc. Biol.* **70**, 950–960.
- Bach, E. A., Aguet, M., Schreiber, R. D. (1997) The IFN  $\gamma$  receptor: a paradigm for cytokine receptor signaling. *Annu. Rev. Immunol.* **15**, 563–591.
- Van Boxel-Dezaire, A. H., Stark, G. R. (2007) Cell type-specific signaling in response to interferon- $\gamma$ . *Curr. Top. Microbiol. Immunol.* **316**, 119–154.
- Kong, X. F., Vogt, G., Itan, Y., Macura-Biegun, A., Szaflarska, A., Kowalczyk, D., Chappier, A., Abhyankar, A., Furthner, D., Khayat, C. D., et al. (2013) Haploinsufficiency at the human IFNGR2 locus contributes to mycobacterial disease. *Hum. Mol. Genet.* **22**, 769–781.
- Fleisher, T. A., Dorman, S. E., Anderson, J. A., Vail, M., Brown, M. R., Holland, S. M. (1999) Detection of intracellular phosphorylated STAT-1 by flow cytometry. *Clin. Immunol.* **90**, 425–430.
- Chappier, A., Kong, X. F., Boisson-Dupuis, S., Jouanguy, E., Averbuch, D., Feinberg, J., Zhang, S. Y., Bustamante, J., Vogt, G., Le-